CREEP AND PRE-STRESSED CONCRETE

by

ATILLA ORHUN

B.S., Robert College, Istanbul, Turkey, 1957

A THESIS

submitted in partial fulfillment of the

requirements for the degree

MASTER OF SCIENCE

Department of Civil Engineering

KANSAS STATE UNIVERSITY
OF AGRICULTURE AND APPLIED SCIENCE

1960

TABLE OF CONTENTS

INTRODUCTION

A Brief History of Prestressed Concrete

Prestressed concrete is almost as old as modern reinforced concrete. However, simplicity of reinforced concrete favored its wider use.

In his patent, "Construction of Artificial Stone and Concrete Pavements" (applied for in 1886), P. H. Jackson of San Francisco described many methods of performing the stretching of ties. This principle was used in the footings of arches along their length by skewbacks, turnbuckles, screws and nuts, wedges, etc.

In the year 1888, another patent was applied for by the German, C. F. W. Doehring, which might be related to prestressing. In this, short members of triangular sections for use as a fire resisting protection for timber floors were manufactured from mortar and tensioned wires.

The idea of counteracting the strain due to loading was clearly expressed, for the first time, by the Austrian, J. Mandl, in 1896, who wanted to utilize the maximum strength of concrete by reducing the tensile stresses under the load. A formula for the magnitude of the stretching force in accordance with this proposal was derived by the German, M. Koenen, in 1907, with the object that the tensile stress of the concrete caused by the working load should be limited to a certain magnitude, assuming a triangular straight line stress distribution.

In the same year, the Norwegian, J. G. F. Lund, suggested the production of straight vaults consisting of rows of prefabricated "brittle" blocks, with prestressed tie-rods arranged between the rows in a wide mortar joint. The compression was transmitted to the blocks by washer plates at the ends, and the bond was destroyed in stretching. Similarly in 1908, the American, G. R. Steiner, proposed to tighten the reinforcing rods, first against the green concrete, thus destroying the bond, and then after the hardening of the concrete to increase the tension. The last two proposals thus represent the first steps towards effective post-tensioning.

However, most of these early attempts failed due to loss of prestress caused by shrinkage and creep. It is clear that the entire prestress becomes ineffective if the initial prestress is not higher than the sum of all losses. In the early attempts, stress losses were not considered to be important. Thus, the first basic step for prestressed concrete was not taken.

The first to suggest the use of high strength steel in connection with pipes was the Austrian engineer, F. Emperger, in 1923.

A further development of prestressing led to the demand for a guaranteed absence of cracks, which can be ensured reliably by "full" prestressing. In this case, the tensioning forces had to be of such magnitude that no tensile stress would occur in the concrete under full working load, even after all possible shrinkage and plastic flow had taken place. R. H. Dill, of Alexandria, Nebr., appears to have been the first, in 1923-25, to propose that this should be carried out by post-tensioning. W. H. Hewett, of Minneapolis, Minn., made suggestions similar to those of Dill, after he had successfully applied his ideas to circular tanks in 1922, in which the structure was not strained by bending but by tensioning only.

Independently of these American ideas, in 1928 the French engineer E. Freyssinet proposed a scheme for creating a new homogenous material from concrete by using high strength steel or wire bonded to the concrete. This allowed such a high prestress that even after losses the residual tensioning force was sufficiently large to cause permanent compressive stresses in the concrete sections of the structure under working load. Moreover, a considerable saving of steel was achieved.

This idea was further developed in Germany by Hoyer in 1938, who introduced the fabrication of prestressed beams in a long, continuous form. They were then cut into pieces of the required length. Such prefabrication was possible previously only with metals.

The practical application of efficient prestressing using high strength wire and high tensile stresses is essentially due to E. Freyssinet. Although R. H. Dill had reached the same conclusions previously, Freyssinet recognized the importance of creep, the influence of which was not formerly appreciated.

Practical applications of prestressed concrete on a large scale started in 1940, following the pre-tensioning method suggested by Hoyer in 1938, and post-tensioning methods suggested in 1939 by Freyssinet and Professor G. Magnel of France.

Purpose of the Research

In the past, experiments were made by Freyssinet and Magnel (10) on various types of reinforcing steel and prestressed concrete beams carrying different loads to determine the long time effects of creep and shrinkage. As a result of their researches estimates of characteristic values (such as stresses, strains, etc.) to be used for design purposes were obtained, but no theory relating the elastic and plastic behavior of the materials to the behavior of the composite structures was presented.

A linearized theory which makes such a relationship has been developed by Professor P. G. Kirmser (8).

The purpose of this research was to compare the theoretical behavior of full-sized prestressed concrete beams to their actual behavior as determined by experiment.

THE LINEARIZED CREEP THEORY

Since the purpose of the theory is to utilize creep and deformation of small specimens to predict behavior of full size specimens, it is evident that these non-elastic deformations are of greatest importance to it.

Creep is the plastic flow of concrete with lapse of time.

Shrinkage is the decrease in the volume of concrete caused by the evaporation of water in the concrete.

It is evident that the separation of creep and shrinkage is difficult. Creep tests are customarily made by measuring the shrinkage specimen and deducting this from the measured total deflection to obtain the creep deflection.

There is no evidence that shows shrinkage under stress is the same as that at zero stress.

In the theory which follows, the creep and shrinkage effects are lumped together to form one function, called the unit creep function which is designated by a(k,t).

For concrete it appears that the major variables are: stress, length of time of loading, and age of concrete at the time of loading. In the equations of the theory stress is noted with the letter (S); the length of time of loading with (t); and the age at the time of loading with (K).

For steel the age of the steel at the time of loading is always such that no change in creep properties will occur. However, this is not true for concrete.

The theory which follows is linear, because it assumes the creep is linearly dependent on stress, thus $a(K,t)$ is the creep per psi., and because it assumes superposition of stresses and deformations.

The theory is approached in stages considering successively more complicated problems.

Assuming that the total unit deformation per psi. is the sum of the elastic strain and the creep gives,

(1) $\delta_1(K,t) = \frac{1}{E} + a(K,t)$,

where $\frac{1}{E}$ is the elastic deformation, and $a(K,t)$ is the creep caused at time t by a 1 psi stress applied at time K.

Let (K,t) = unit strain at time, t caused by a stress, S applied at time, K.

(2) $\delta(t) = \sum_i \frac{S(K_i)}{E} + \sum_i S(K_i)\, a(K_i,t)$.

Since $\sum_i S(K_i) = S(t)$, (2) can be written

(3) $\delta(t) = \frac{S(t)}{E} + \int_{K=0}^{t} \frac{\partial S}{\partial K} a(K,t)dk$ for differentiable $S(K)$ or

(4) $\delta(t) = \frac{S(t)}{E} + \int_{K=0}^{t} \frac{\partial S_o}{\partial K} a(K,t)dK + \sum_i [S(J_i+) - S(J_i-)]a(J_i,t)$,

where there are finite jumps in the applied stresses at times J_i. Here $\frac{S_o}{K}$ applies only to the differentiable part of S. This formula can be put in a different form by integration by parts.

Consider $\int_o^t \frac{\partial S_o}{\partial K} a(K,t)dk$

then integration by parts gives

$$\int_0^t \frac{\partial S_o}{\partial K} a(K,t)dk = S_o(K)\ a(K,t)\ \Big]_o^t - \int_o^t S_o(K)\ \frac{\partial a(K,t)}{\partial K}\ dk$$

$$= S_o(t-)a(t,t) - S_o(0+)a(0,t) - \int_o^t S_o(K)\frac{\partial a(K,t)}{\partial K}\ dk.$$

Now $S_o\ (0+) = 0$, and $a(t,t) = 0$

therefore (4) becomes

(6) $$\delta(t) = \frac{S(t)}{E} - \int_o^t S_o(K)\ \frac{\partial a(K,t)}{\partial K}\ dk + \sum_i [S(J_i+) - S(J_i-)]a(J_i,t)$$

This formula may be confusing, for the function S may be differentiable, except with a finite number of jumps of finite height, where S_o is only the differentiable part of this function S.

This confusion may be cleared up by again considering (4), and replacing S_o in the integral by S. Then care must be used in integrating by parts.

Consider a function S with one jump at J_1. Then (4) becomes

(7) $$\delta(t) = \frac{S(t)}{E} + \int_o^{J_1} \frac{\partial S}{\partial K}\ a(K,t)dk + \int_{J_1}^t \frac{\partial S}{\partial K}\ a(K,t)dk$$

$$+ \left[S(J_1+) - S(J_1-)\right]\ a(J_1,t)$$

in which S is differentiable $0 < K < J_1$ and $J_1 < K < t$.

Integrating these by parts separately gives

$$\int_o^{J_1} \frac{\partial S}{\partial K}\ a(K,t)dk = S(K)a(K,t)\Big]_o^{J_1} - \int_o^{J_1} (S(K)\ \ \frac{\partial a}{\partial K}\ dk$$

$$= S(J_1-)a(J_1-,t) - S(0+)\ a(0+,t) - \int_o^{J_1} S(K)\ \frac{\partial a}{\partial K}\ dk\ ,$$

and

$$\int_{J_1+}^{t-} \frac{\partial S}{\partial K}\, a(K,t)dk = S(t-)a(t-,t) - S(J_1+)a(J_1+,t) - \int_{J_1+}^{t} S(K)\, \frac{\partial A}{\partial K}\, dk$$

then (7) becomes

$$(8)\quad \delta(t) = \frac{S(t)}{E} + S(J_1-)a(J_1-,t) - S(0)a(0,t) - \int_{0}^{J_1-} S(K)\, \frac{\partial a}{\partial K}\, dk$$

$$-S(J_1+)a(J_1+,t) - \int_{J_1}^{t} S\, \frac{\partial a}{\partial K}\, dk + \left[S(J_1+) - S(J_1-)\right]a(J_1,t).$$

Since a(K,t) is a continuous function, it follows that

$$(9)\quad \delta(t) = \frac{S(t)}{E} - \int S(K)\, \frac{\partial a(K,t)}{\partial K}\, dk$$

where S(t) is a differentiable function except for a finite number of finite jumps.

Actually, for any "reasonable" problem involving an actual structure S(t) will not have jumps. However, for sudden changes in loading it may be a good approximation to take S(t) as a jump function.

This formula is applied to a number of problems below.

Problem 1: Given a pre-stressed member, find the stress in the steel and concrete. Assume the loads are applied at K = 0, and the member is symmetrical.

Summing the forces along the axis

$$S_s A_s = S_c A_c$$

where S_s and S_c are stresses in steel and concrete. S_c and A_c are the areas of steel and concrete.

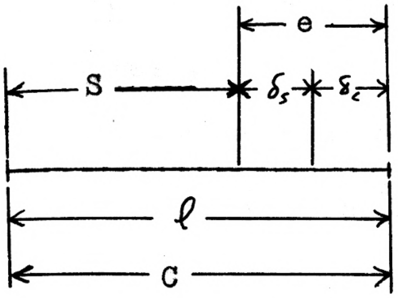

From equation (9)

$$S(t) = \frac{S_s(t)}{E} - \int_0^t S_s(K)\,\frac{\partial a(K,t)}{\partial K}\,dk,$$

the length of the steel is the same as the length of the concrete. Thus,

$$\ell_s + \delta_s \ell_s = \ell_c - \delta_c \ell_c,$$

and since

$$\ell \simeq \ell_s \simeq \ell_c,$$

(10) $$\ell\delta_s = e - \delta_c \ell .$$

Equation (9) becomes, on substitution into (10)

$$\frac{S_s(t)\ell}{E_s} - \ell\int_0^t S_s(K)\frac{\partial a_s}{\partial K}\,dk = e - \frac{\ell S_c(t)}{E_c} + \ell\int_0^t S_c(K)\frac{\partial a_c}{\partial K}\,dk .$$

Using $S_s A_s = S_c A_c$, this is

$$\frac{\ell S_c A_c}{A_s E_s} - \ell\int_0^t \frac{S_c A_c}{A_s}\frac{\partial a_s}{\partial K}\,dk = e - \frac{\ell S_c}{E_c} + \int_0^t S_c\frac{\partial a_c}{\partial K}\,dk,$$

or

(11) $$S_c(t)\ \frac{A_c\ell}{A_s E_s} + \frac{\ell}{E_s} = e + \ell\int_0^t S_c\ \frac{\partial a_c}{\partial K} + \frac{A_c}{A_s}\frac{\partial a_s}{\partial K}\ dk .$$

In this work the term $(\frac{A_c}{A_s}\ \frac{a_s}{K})$ is very small (Dill's work) (5), and therefore neglected.

Then

(12) $$S_c(t)\ \frac{A_c\ell}{A_s E_s} + \frac{\ell}{E_c} = e + \ell\int_0^t S_c\ \frac{\partial a_c}{\partial K}\,dk .$$

Solving (11) gives $S_c(t)$. $S_s(t)$ is given in terms of this solution by

(13) $$S_s(t) = \frac{A_c}{A_s}\,S_c(t) .$$

Problem 2: Given a member whose deformation is specified, find the stress.

In this case (9) is

$$(\quad -b) \quad \delta(t) = \frac{S(t)}{E} - \int_0^t S(K) \frac{\partial a}{\partial K} \, dk ,$$

with the unknown function S(t).

Thus,

$$(14) \quad S(t) = E\,\delta(t) + E\int_0^t S(K) \frac{\partial a}{\partial K} \, dk .$$

Problem 3: Given a reinforced concrete beam, pre-stressed or not, find the stress in the concrete assuming the stress in the steel is known.

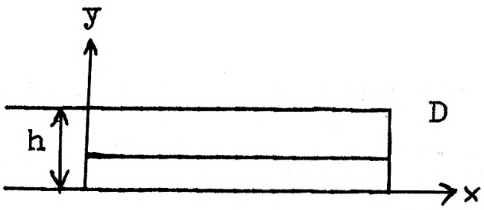

Notations:

$M(x)$ = moment at x

h = depth of beam

D = distance of steel from the bottom

C_o = force in the steel

$S(y,t)$ = stress at y at time t.

$\bar{y}$ = neutral axis

A_c = area of concrete

E_c = modulus of elasticity of concrete

The equations describing the problem are, for a given x, relating stress and deformations

$$(15) \quad S_c(y,t) = E_c\delta_c(y,t) + E_c\int_0^t S_c(y,t) \frac{\partial a}{\partial K} \, dk ,$$

equating moments

(16) $\int y \, S_c(y,t) \, dA - DS_sA_s = M(x),$

stating that planes remain planes

(17) $$\delta c(y,t) = C_1(t) + C_2(t)y \quad ,$$

and summing horizontal forces

$$\int S_c(y,t)dA = C_o \quad .$$

The solution of these equations for S_c follows. Multiplying (15) by dA, substituting (17), and integrating, yields

(19) $$\int_{A_c} S_c(y,t)dA = E_c \int_{A_c} [C_1(t) + C_2(t)y] \, dA$$
$$+ E_c \int_o^t \int_{A_c} S(y,K) \, \frac{\partial a(K,t)}{\partial K} \, dk \, dA$$

which is

(20) $$C_o = E_cA_c \, C_1(t) + E_cC_2(t) \, \bar{y} \, A_c + E_cC_o \int_o^t \frac{\partial a_c}{\partial K} \, (K,t) \, dk \quad .$$

Now multiplying (15) by y and integrating over A_c gives

(21) $$\int_{A_c} y \, S_c(y,t)dA = \int_{A_c} [E_cC_1(t) + E_cC_2(t)y] \, y \, dA$$
$$+ E_c \int_{A_c} \left[\int_o^t S_c(y,K) \, \frac{\partial a}{\partial K} \, dk \right] ydA \quad .$$

Thus,

(22) $$M(x) + C_oD = E_c\bar{y} \, A_cC_1(t) + E_cI_cC_2(t)$$
$$+ E_c [M(x) + C_oD] \int_o^t \frac{\partial a(K,t)}{\partial K} \, dk \quad .$$

Solving (20) and (22) leads to

(23) $$C_1(t) = \frac{1 + E_c a_c(0,t)}{E_c A_c} \frac{\begin{vmatrix} C_o & \bar{y} \\ M_x + C_o D & h^2 \end{vmatrix}}{\begin{vmatrix} 1 & \bar{y} \\ \bar{y} & k^2 \end{vmatrix}}$$

or

(23-b) $$C_1(t) = \frac{1 + E_c a_c(0,t)}{E_c A_c} \cdot \frac{C_o h^2 - \bar{y} M_x - \bar{y} C_o}{k^2 - \bar{y}^2} ,$$

and

(24) $$C_2(t) = \frac{1 + E_c a_c (0,t)}{E_c A_c} \frac{\begin{vmatrix} 1 & C_o \\ \bar{y} & M_x + C_o D \end{vmatrix}}{\begin{vmatrix} 1 & \bar{y} \\ \bar{y} & k^2 \end{vmatrix}}$$

or

(24-b) $$C_2(t) = \frac{1 + E_c a_c(0,t)}{E_c A_c} \cdot \frac{M_x + C_o D - \bar{y} C_o}{k^2 - \bar{y}^2} .$$

The deflections are found by substituting these values for the constants of equation (17), which gives

(25) $$\delta_c(y,t) = \frac{1 + E_c a_c (0,t)}{E_c A_c (k^2 - \bar{y}^2)} \Big[(C_o k^2 - \bar{y} M_x - C_o \bar{y} + (M_x + C_o D - \bar{y} C_o) y \Big]$$

or

$$\delta_c(y,t) = \frac{1 + E_c a_c (0,t)}{E_c A_c (k^2 - \bar{y}^2)} \left[C_o (k^2 - D\bar{y} + Dy - \bar{y} y) + M_x (y - \bar{y}) \right].$$

Thus,

(26) $$S_c(y,t) = \delta_c(y,t) E_c + E_c \int_0^t S_c(y,k) \frac{\partial a_c(K,t)}{\partial K} dk .$$

To find the deflection curve, note that

(27) $$\frac{\partial^2 y}{\partial x^2} = \frac{-C_1 + (C_1 + C_2 h)}{h} = C_2(t) .$$

If $a(0,t) = C_o = 0$, the usual deflection equation should be obtained. Putting $C_o = 0$ in (27) gives

$$\frac{\partial^2 y}{\partial x^2} = \frac{1}{EA}\,\frac{M_x}{k^2 - y^2} = \frac{M(x)}{E(Ak^2 - A\bar{y}^2)} = \frac{M(x)}{EI_{c.g.}} ,$$

which is the usual equation for the elastic deflection of beams.

Problem 4: Given Problem 3. Find the force, C_o, in the steel assuming the initial force, F, is not known.

Notations:

F = initial force on the steel

$$R = \frac{1 + E_c\ a_c\ (0,t)}{E_c A_c\ (k^2 - \bar{y}^2)}\ E_s\ A_s$$

K = radius of gyration

$\Delta(t)$ = lateral deflection of midpoint at time t

L = length of the beam

= radius of curvature of the beam

According to (18),

$$\int s_c(y,t)\,dA = C_o\ .$$

Summing the horizontal forces on steel gives

(28) $$C_o = F - \delta_c\ E_s\ A_s\ ,$$

where

(17) $$\delta_c(y,t) = C_1(t) + C_2(t)y \quad \text{and where} \quad y = D\ .$$

Substituting (17),

(29) $$C_o = F - (C_1 + DC_2)\ E_s A_s\ .$$

Substituting C_1 and C_2 from (23) and (24) gives

$$C_o = F - \frac{1 + E_c a_c(0,t)}{E_c A_c(k^2 - \bar{y}^2)} \quad E_s A_s \left[C_o k^2 - \bar{y} M(x) - \bar{y}\, D\, C_o + M(x)\, D + C_o D^2 - \bar{y}\, D\, C_o \right] \tag{30}$$

Simplifying (30) yields

$$C_o = F - R\,(k^2 - 2\bar{y}\, D + D^2)\, C_o - R\,(D - \bar{y})\, M(x) \tag{31}$$

Finally,

$$C_o = \frac{F - R\,(D - \bar{y})\, M(x)}{1 + R\,(k^2 - 2\bar{y}\, D + D^2)} \tag{32}$$

PROCEDURE AND DESCRIPTION OF THE TESTS

Construction of the Test Specimens

To carry out the experiment the following specimens were cast from the same batch of ready mix concrete. The mix proportions and properties are given in Table 1 and Table 2 of the Appendix.

1. Two (8" x 16" x 21' 4") beams with 10 prestressing cables, considerably offset from the center of the beam with two keeper bars at the top of the beam (beam No. 1, Fig. 1)
2. An (8" x 16" x 21' 4"), prestressing-control beam with 10 prestressing cables axially placed in the concrete. (beam No. 2, Fig. 1)
3. An (8" x 16" x 21' 4"), non-prestressed, shrinkage control beam with only 4 keeper wires to support the weight of the beam. (beam No. 3, Fig. 1)
4. Five small (3" x 4" x 16"), concrete specimens. (Fig. 2)

The two full-sized beams (beam No. 1) were prepared for deflection and strain measurements after being loaded. Nine sets of reference marks at the opposite sides were placed along the middle of the beam for deflection measurements. Three sets of plugs on opposite sides of the beam were placed to measure the strain with a Whittemore strain gage. (Fig. 1, Appendix)

Beam No. 2, with the prestressing wires placed axially, was prepared to measure the strains. Three sets of plugs on opposite sides of the beam were placed for this purpose. (Fig. 2,

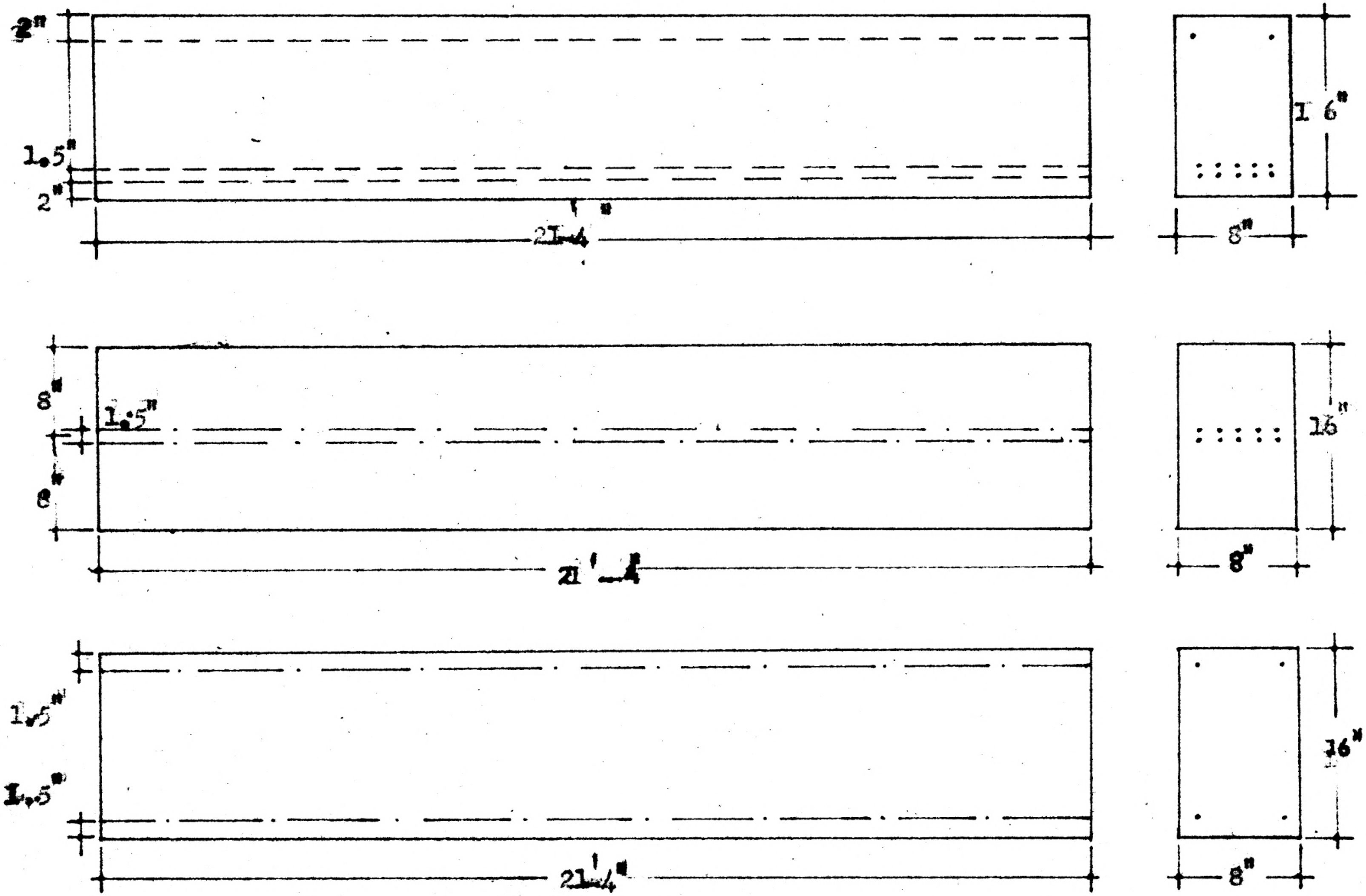

Fig.1b. Large specimens.

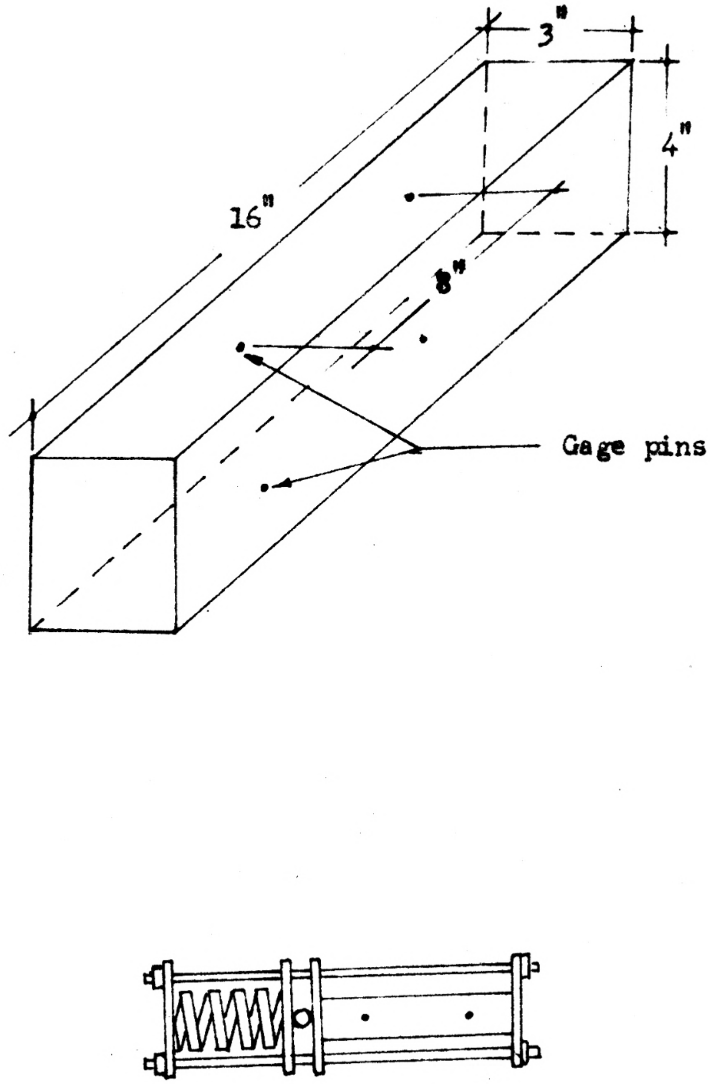

Fig. 2. (3" x 4" x 16") specimens

Appendix)

The third full-sized beam (No. 3) was prepared for measuring shrinkage. The plugs were set in locations similar to those of beam No. 2. (Fig. 2, Appendix)

Of the three small specimens (3" x 4" x 16"), one was prepared for measuring shrinkage with no loads applied. The other two were loaded axially by means of heavy springs. These specimens had a set of plugs on each of two opposite sides for strain measurements. (Fig. 3)

The full-sized beams (8 x 16 x 21' 4") were cast in place on a heavy wooden frame two feet above the floor, with their 16-inch sides vertical. After the prestressing wires were released, the forms were removed and the beams were placed with their 8-inch sides vertical in order to permit the strains to be read from above and below. There were two main reasons for this arrangement. 1. The Whittemore strain gage used functioned well on pins set in horizontal surfaces, but did not give consistent readings with pins set in vertical surfaces. 2. The plan of loading one concrete beam against the other necessitated the use of a horizontal position for the beams.

The main problem in carrying the experiment out was that of supporting the large forces involved in holding the prestressing wires. In each beam (except the non-prestressed, shrinkage control beam) there were ten prestressing cables under a total tension of 140,000 lbs. In commercial production of pretensioned beams, large anchors are used at each end to hold the wires.

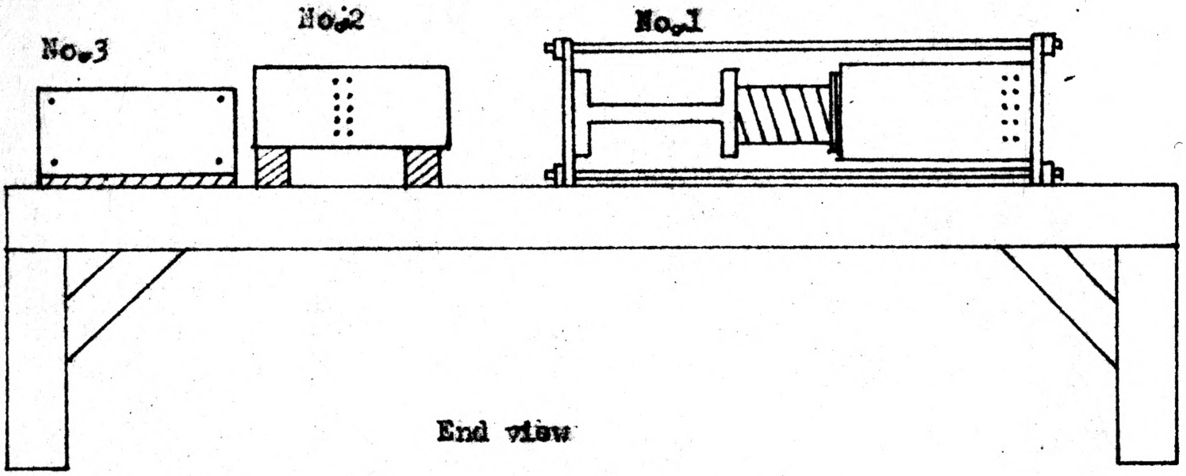

End view

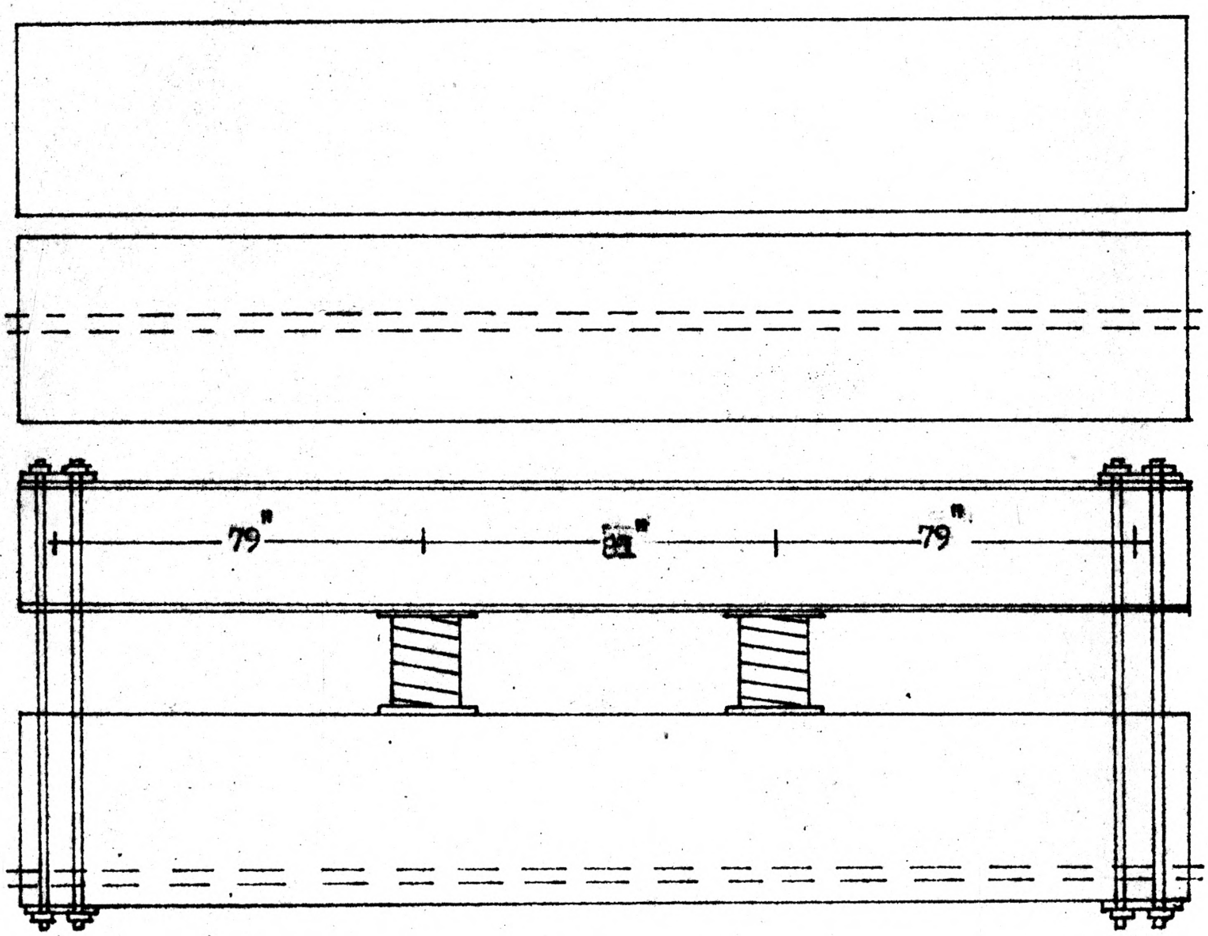

Top view

Fig.3 Set-up of the large beams.

However, no possibility of using anchors existed here, so the problem was solved by using eight (4" x 12" x 24' 0") bridge planks as columns to hold heavy crossheads. The wires were anchored to these crossheads, and were tensioned to a force of 140,000 lbs. 48 hours before pouring the concrete.

In addition to serving as the supporting columns for the prestressing cables, the bridge planks were lined with plywood and served as the forms for the beams.

Twenty-two days after casting, the wires were released and the forms removed. It was observed that a shear failure had occurred on the top row of prestressing wires of one of the active beams (beam No. 1-A). This beam was broken up and discarded.

Fourteen days after the casting, the planks of prestress-control beam (beam No. 2) sheared off diagonally. This released the wires on this specimen, but caused no damage to the beam.

A steel I-beam was substituted for the broken active beam (beam No. 1-A). Thus the remaining active beam was loaded against the steel I-beam. This loading was accomplished by placing heavy springs at the third points between the I-beam and the concrete beam, and pinching the ends together with the aid of a hydraulic jack and some special steel clamps, as shown in Fig. 3.

The forces necessary for loading this beam were not applied at once. They were applied as follows: 4000 lbs.; 7600 lbs.; 11,500 lbs. These were the forces applied at each end of the beam.

Two of the small specimens (3" x 4" x 16") were loaded to 1000 psi, and one to 1500 psi by means of heavy springs and special clamps as shown in Fig. 2.

Two specimens were prepared for measuring shrinkage, and were not loaded.

Data Recorded

On active beam (Bm. No. 1) vertical deflections parallel to the vertical forces caused by springs were recorded. Longitudinal deflections or elongations were also recorded.

On the pre-stress control beam (Bm. No. 1) longitudinal and vertical deflections were recorded.

On the non-pre-stressed, shrinkage control beam (Bm. No. 3) only elongations or longitudinal deflections were recorded.

On the small specimens (3" x 4" x 16") only elongations were recorded.

The data is tabulated in the Appendix.

Measurements and Calculations

In measuring the deflections a nylon string was placed with its ends in the center groove of the end pins, and was tightened. After this step, the end of a 1/50th scale was placed just touching the string. The distance to the mark was estimated to the nearest 1/100th of an inch.

In measuring strains, a Whittemore 0.0001" gage was used.

Prior to measurements both gage and zero bar were allowed to stand by the specimen for about 30 minutes, so that temperature equilibrium would be reached.

Then the gage was rocked back and forth on the gage pins until a consistent maximum reading was obtained.

Strains were obtained by dividing the difference between the "new readings" and the "original readings" by 8. The strains at corresponding stations on opposite sides of the beam were averaged, (i.e., $\frac{A+B}{2}$, $\frac{C+D}{2}$, $\frac{E+F}{2}$, etc.)

The original readings for the beams were taken 22 days after the beams were cast. For the small specimens the original readings were made 18 days after being cast.

The strain readings were corrected by converting them to 80°F.

In the case of the small specimens, pure creep was obtained by subtracting the average shrinkage from the gross creep. (See Appendix, Table -7.)

After each periodical measurement stresses on active beam (Bm. No. 1) were corrected to their original values, if any stress loss was observed. This was done by placing a hydraulic jack on the springs at each end of the beam, then adjusting the clamping bolts until the original stresses were restored.

The forces on the small specimens were also corrected to their original values after each periodical measurement. This was done by putting the assembly under a testing machine and applying a force equal to the original, then readjusting the bolts on the clamps until they were fingertight.

THE NATURE OF CREEP

The nature of creep has been investigated by Shank (13), Arnan (2), Reiner (2), Ross (12), Teinowitz (2), Cowan (3), Lorman (9), Freudenthal (6), and Vidal and Meissner (7).

Of these investigations, the works of Lorman, Freudenthal, and Vidal and Meissner have the greatest importance for the research reported here.

Lorman presented the empirical formula for fitting experimental creep data which is later used in this thesis.

Freudenthal made numerous tests to study the creep-recovery and response of concrete to loading and unloading cycles. According to Freudenthal (6),

> "Concrete is formed by an aggregation of loose grains of sand and aggregate held together by a highly viscous liquid, the cement paste. The viscosity of this liquid increases with time as a result of chemical changes within the structure (crystallization) until a complete crystalline network blocks all viscous deformation.
>
> "Hardened cement paste is essentially a non-linear Maxwell body of high viscosity and cohesion. The aggregates and sand form a noncohesive, granular mass, the resistance of which to irrecoverable deformation by shear (in this case identical with gliding-rupture) is the result of friction between the grain, which in turn is a function of the applied hydrostatic pressure."

From these statements it can be concluded that concrete is highly plastic in its early stages, and that as it gets older its plasticity decreases and it becomes practically an elastic material.

E. N. Vidal and H. S. Meissner of the U. S. Reclamation

Bureau made a 10-year study of the creep properties of the concrete used to build Shasta Dam (7). Their studies verify Freudenthal's conjectives, and they present the three dimensional graph shown in Fig. 4, showing the elastic and plastic deformations of the Shasta Dam concrete as a function of age of loading and duration of application of the load.

On the basis of Lorman's and Vidal and Meissner's work it was assumed that an empirical formula of the form

$$a\,(k,t) = a_1(k)a_2(t)$$

could be fitted to the experimental data. (Fig. 7)

In the research of this thesis, all the small creep specimens were loaded at the same age. Therefore, no creep surface could be constructed from direct experimental data. The method of Lorman was used to determine $a_2(t)$, and $a_1(k)$ was found by assuming the effect of age at time of loading to be the same as that of the Shasta Dam concrete as shown in Fig. 5.

According to Ross and Lorman (9), the empirical formula

$$a(t) = \frac{mt}{n + t}$$

fits experimental creep data for concrete very well. In this formula m and n are the slope and intercept of the best straight line fit of the experimental creep data when graphed with $V = \frac{st}{e_c}$ as absissa and t as ordinate. In the formula for V s is the stress applied, t is the time elapsed since loading, and e_c is the creep deformation.

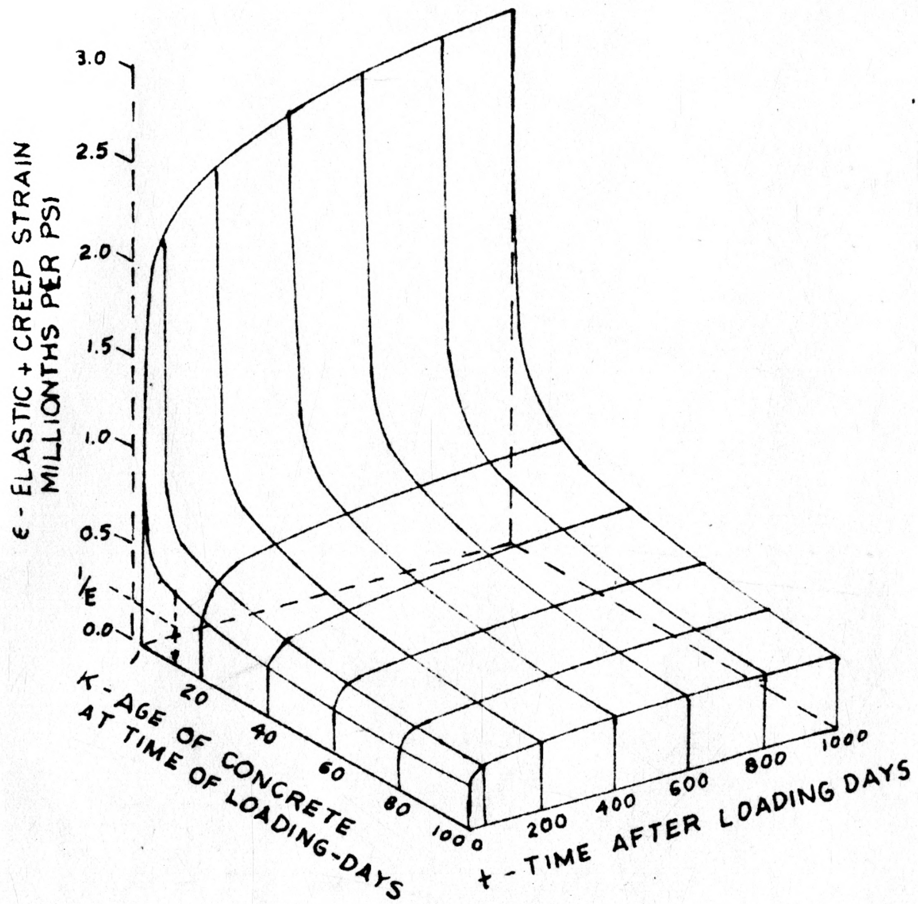

Fig.4. A three dimensional creep surface

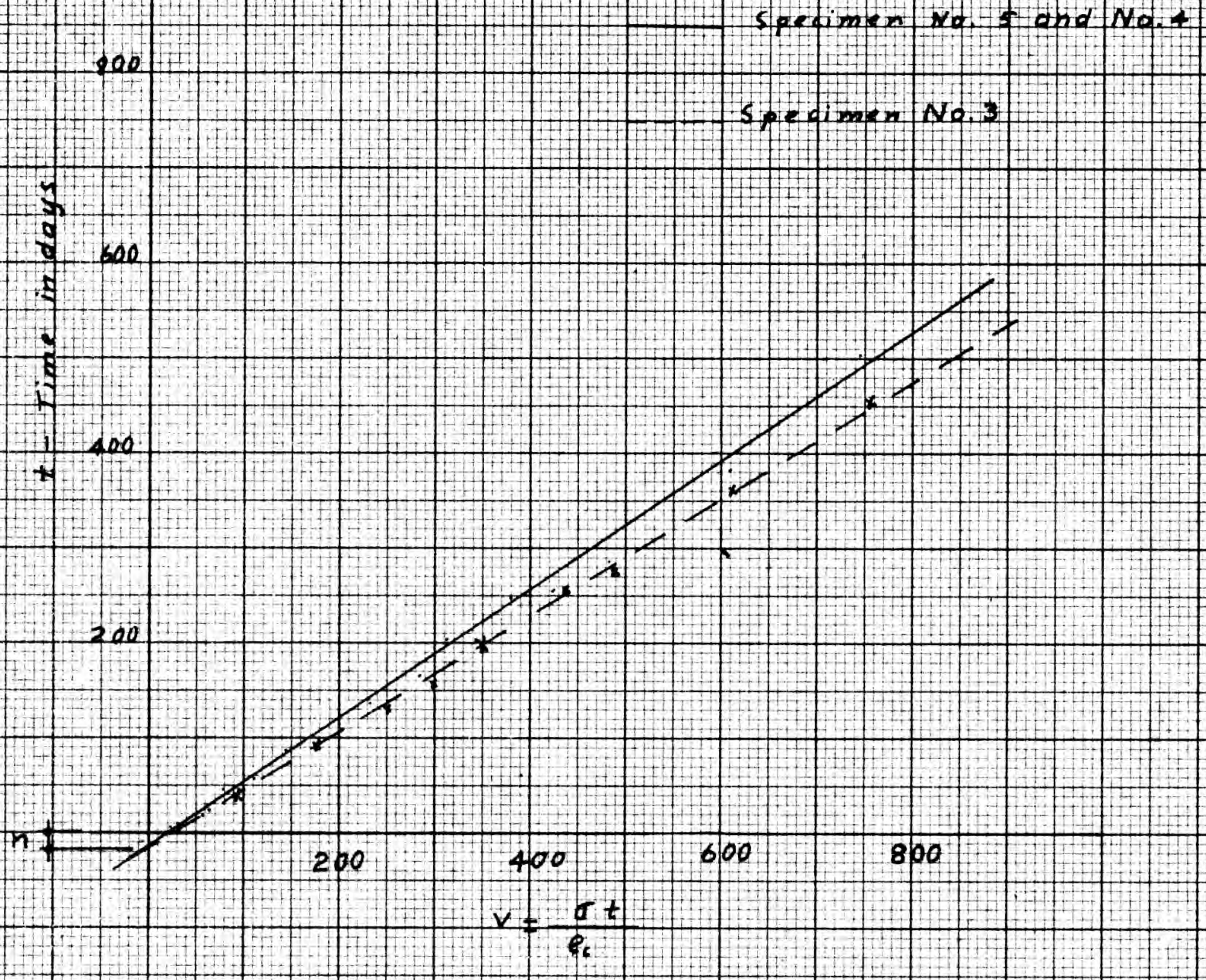

m = slope of the line
n = intercept of the line on vertical axis

Fig. 5. Evaluations of the constants for Lorman's formula

Fig. 6 shows the experimental data for specimens 3, 4, and 5 graphed according to this procedure, using the measured values shown in Fig. 5. The average values of m and n found in this manner are $m = 0.603$ and $n = 18$, respectively. Thus, the Ross-Lorman formula for the Walters Company Concrete used in this experiment is

$$(34) \qquad a_2(t) = \frac{0.603t}{18 + t} \quad ,$$

where $a_2(t)$ is the creep in 10^{-6} in. per psi. This formula holds strictly for concrete which is 18 days old at the time of initial loading.

From Fig. 7, which shows the creep of the Shasta dam concrete, it is seen that the variation of creep with age k of the concrete at time of initial loading can be approximated by

$$(35) \qquad a_1(k) = \frac{k + 26}{4k} \times 10^{-6} .$$

Assuming that the creep surface for the Walters Company concrete used in the research reported here varies similarly, it can be represented by

$$(36) \qquad a(k,t) = C \, \frac{k + 26}{4k} \, \frac{.603 \; t}{18 + t} \, 10^{-6}$$

where the constant C is to be evaluated so that $a(18,t)$ fits the experimental creep data obtained here. Thus,

$$(37) \qquad 1 = C \, \frac{18 + 26}{4(18)} \quad ,$$

$$\text{or} \qquad C = \frac{72}{44} \quad .$$

In the analytic investigations it is convenient to measure

Fig. 6. Experimental and theoretical creep curves for specimens 3,4, and 5.

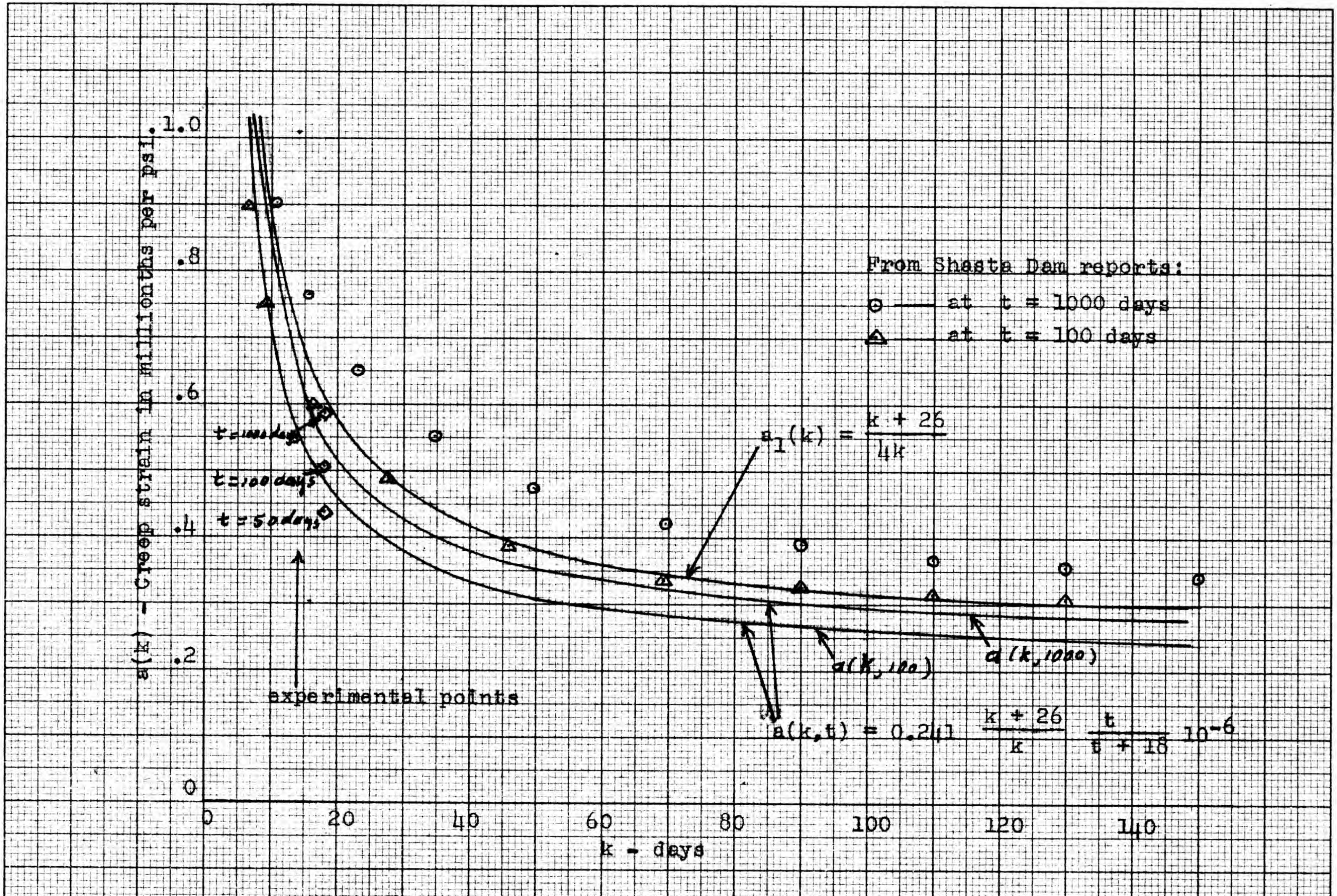

Fig. 7. Creep as a function of age of concrete at initial loading.

the age of the concrete from the time of initial loading. Therefore, the k axis was shifted by letting $k = K + 18$.

The creep function so obtained is

$$a(K,t) = 0.241 \frac{K + 44}{K + 18} \frac{t}{t + 18} \times 10^{-6} \quad . \tag{38}$$

This function is compared to the Shasta Dam data in Fig. 7, and the experimental creep data for $k = 18$ $(K = 0)$ is also shown in Fig. 7.

DESIGN OF THE ACTIVE BEAM

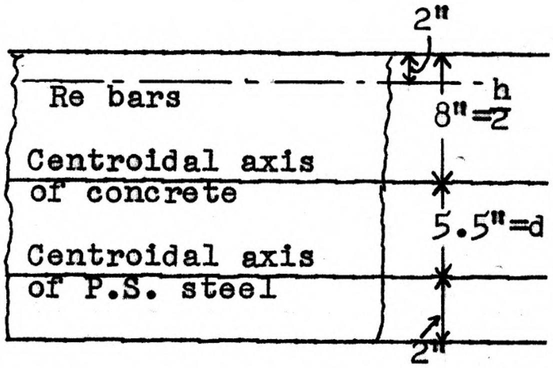

When P.S. wires released

Steel strain -

$$S = \frac{P}{A}, \quad S = eE$$

$$e_c = \frac{P}{E_c A_c}$$

From Eccent. Loading -

$$S_c = \frac{Mc}{I} \quad \frac{Pd \times d}{I_c} \quad \frac{Pd^2}{I_c}$$

$$e_c = e_s = \frac{S_c}{E_c} = \frac{Pd^2}{E_c I_c}$$

Total Steel Strain

$$e_s = \frac{P}{A_c E_c} + \frac{Pd^2}{E_c I_c} =$$

$$\frac{P}{E_c} \quad \frac{1}{A_c} + \frac{d^2}{I_c}$$

Stress Loss in Steel = $e_s E_s$

$$e_s E_s = \frac{PE_s}{E_c} \quad \frac{1}{A_c} + \frac{d^2}{I_c}$$

Also stress Loss =

$$\frac{F_s - P}{A_s} = \frac{PE_s}{E_c}\left[\frac{1}{A_c} + \frac{d^2}{I_c}\right]$$

Symbols

b = width of beam

h = depth of beam

l = dist. from rebars to top of beam

A_c = transformed area of concrete and rebars

A_s = area of prestressing steel

A_{rb} = area of rebars

E_c = modulus of elasticity of concrete

E_s = modulus of elasticity of steel

I_c = transformed moment of inertia of concrete rebars

I_t = transformed moment of inertia of concrete, rebars, and prestressing wires

r = distance from transformed centroid (for I_t) to bottom of beam

d = eccentricity of P.S. steel

P = force in P.S. steel just after wires cut

P_F = final force in P.S. steel after beam loaded

e_s = strain in P.S. steel

e_c = strain in concrete

S_s = stress in P.S. steel

S_c = stress in concrete

Finally,

$$P = \frac{F_s}{1 + \frac{A_s E_c}{E_c}\left[\frac{1}{A_c} + \frac{d^2}{I_c}\right]} \quad .$$

Using the data form beam No. 1,

$$F_s = 130{,}000 \text{ (orig. } 140{,}000 - 10{,}000)$$

$$A_s = 0.799 \ (0.0799 \times 10)$$

$$E_s = 27 \times 10^6$$

$$E_c = 130.62$$

$$d = 5.5''$$

$$I_c = 2821$$

gives

$$P = \frac{130{,}000}{1 + \frac{.799 \times 27 \times 10^6}{4.05 \times 10^6}\left[\frac{1}{130.62} + \frac{30.2}{2821}\right]}$$

$$= \frac{130{,}000}{1 + 5.32 \times 0.01835}$$

$$P = 118{,}500 \text{ lbs.}$$

This force is P.S. wires after transfer of P.S., but before any bending load is applied to beam.

The maximum tensile stress in the concrete at the top of the beam is

$$S_c = \frac{M\,\frac{h}{2}}{I_c} - \frac{P}{A_c} = \frac{Pdh}{2I_c} - \frac{P}{A_c}$$

$$= \frac{118{,}500 \times 5.5 \times 8}{2821} - \frac{118{,}500}{130.62}$$

$$= 1850 - 908 = 942 \text{ psi.}$$

Similarly, the maximum compressive stress in the concrete at the bottom of the beam is

$$S_c = -\frac{M\frac{h}{2}}{I_c} - \frac{P}{A_c}$$

$$= - 1850 - 908 = - 2758 \text{ psi} \quad .$$

Since the expected tensile stress was more than the tensile strength of the concrete, two 1/2 inch D reinforcing bars were cast in the top of the beam two inches below the surface.

The transformed moment of inertia of concrete, rebars, and pre-stressing wires were

$$I_t = 2985 \text{ in.}^4 \quad ,$$

and r, the transformed centroid, was found to be 7.97" from the bottom.

The moment to be applied to the center section is calculated as follows:

$$S_c = \frac{Mr}{I_t}$$

$$S_c = 2792 \qquad r = 7.97 \qquad I_t = 2985$$

$$S_c = 2792 = \frac{M\ (7.97)}{2985}$$

$$M = 1{,}045{,}000 \text{ in - lb.}$$

This is the moment needed in the center section to barely eliminate all the stresses in the bottom fiber of concrete. However, to eliminate any chance of the failure of this beam, it was decided to use a moment of 920,000 in-lb. in loading the beam.

From the proposed loading diagram shown below, it is evident that forces F = 11,500 lbs. will provide this bending moment.

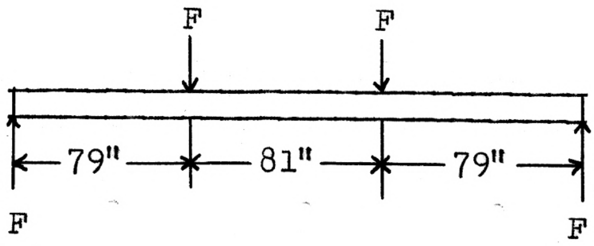

For this loading, the final stress at the top of the beam is

$$S_c = \text{stress from spring load - stress after wires cut}$$

$$= \frac{M(h - r)}{I_t} + 923$$

$$= - \frac{.920 \times 10^6 \times 8.03}{2985}$$

$$= - 2450 + 923 = - 1527 \text{ (comp.)}$$

COMPARISON OF THEORY TO EXPERIMENT

Analysis of the Axially Pre-stressed Beam

Since the equation for creep (32) was found, it was possible to analyze No. 2 beam, which was pre-stressed axially with no external loading.

According to (eq. 12) stress as a function of time is

$$S_c(t)\left[\frac{A_c \ell}{A_s E_s} + \frac{\ell}{E_c}\right] = e + \ell \int_0^t S_c \frac{\partial a_c}{\partial k}\, dk \quad . \tag{12}$$

However, since there was no possible way of measuring the stresses, (eq. 14) was used by means of which deflection can be calculated.

$$\delta(t) = \frac{S(t)}{E} - \int_0^t S(K) \frac{\partial a}{\partial k}\, dk \quad , \tag{9-b}$$

where

$\delta(t)$ = strain as a function of time,

$S(t)$ = stress as a function of time,

E = elastic modulus of concrete,

$S(K)$ = stress as a function of K,

a_c = creep function which for concrete is

$$a_c(K,t) = .241 \times 10^{-6} \; \frac{K + 44}{K + 18} \; \frac{t}{t + 18} \quad ,$$

and

$$\frac{\partial a}{\partial k} = -7.23 \times 10^{-6} \; \frac{1}{(K + 18)^2} \cdot \; \frac{t}{t + 18} .$$

Let $\frac{S(t)}{E} = C_1$ and $7.23 \times 10^{-6} = C_2$, then (eq. 14) becomes

$$(39)\quad \delta(t) = C_1 + C_2 \int_0^t S(K) \frac{1}{(K + 18)^2} \frac{t}{t + 18} \, dk \; .$$

Although this integral equation is difficult to solve, maximum and minimum bounding functions can be obtained easily.

It is evident that creep increased for increased stress. Therefore, substitution of $S(0)$ into the integral equation (39) will yield a $\delta(t)$ smaller than the true value because $S(0)$ is greater than $S(t)$. Thus (39) is replaced by

$$(40)\quad \delta(t)_{min} = C_1 + C_2 \, S(0) \int_0^t \frac{1}{(K + 18)^2} \frac{t}{t + 18} \, dk \leq \delta(t).$$

Integrating (40) gives in turn

$$(41)\quad \delta(t)_{min} = C_1 + C_2 \frac{S(0)t}{t + 18} \int_0^t \frac{dk}{(K + 18)^2} \; ,$$

$$\delta(t)_{min} = C_1 - C_2 \, S(0) \frac{t}{t + 18} \left. \frac{1}{k + 18)} \right|_0^t \; ,$$

$$\delta(t)_{min} = C_1 + C_2 \, S(0) \frac{t}{t + 18} \frac{1}{18} - \frac{1}{t + 18} \; ,$$

and

$$(42)\quad \delta(t)_{min} = \frac{S(t)}{E} + S(0) \frac{C_2}{18} \frac{t}{t + 18} - C_2 \frac{t}{(t + 18)^2} \; .$$

Similarly creep is decreased for decreased stress, therefore substitution of

$$S(t)_{min} = S(0) \left[1 - \frac{C_2}{18} \frac{t}{t + 18} + \frac{C_2 \, t}{(t + 18)^2} \right] \leq S(t)$$

for $S(t)$ in (39) will yield a value of $\delta(t)$ greater than the true value, because the stress is less than the true value.

Thus,

$$(43) \quad \delta(t)_{max} = C_1 - C_2\ S(0)\ \frac{t}{t + 18} \int_0^t \left[1 - \frac{C_2}{18} \frac{k}{(K + 18)} + \frac{C_2\ t}{(t + 18)^2} \right] \frac{dk}{(K + 18)^2} .$$

Integration and simplification of (43) gives

$$(44) \quad \delta(t)_{max} = C_1 + C_2\ S(0)\ \frac{t}{t + 18} \left[- \frac{1}{K + 18} \quad \frac{C_2}{18} - \frac{C_2}{2} \frac{1}{(K + 18)^2} + \frac{C_2}{2} \frac{k}{(K + 18)^3} + \frac{3\ C_2}{(K + 18)^3} \right]_0^t ,$$

and

$$(45) \quad \delta(t)_{max} = C_1 + C_2\ S(0)\ \frac{t}{t + 18} \left[\left(\frac{C_2}{18} - 1 \right) \frac{1}{t + 18} - \frac{C_2}{2} \frac{1}{(t + 18)^2} + \frac{C_2}{2} \frac{(t + 6)}{(t + 18)^2} - \frac{C_2}{(18)^2} + \frac{1}{18} + \frac{C_2}{2(18)^2} - \frac{3\ C_2}{(18)^3} \right] ,$$

where

$$C_1 = \frac{S(t)}{E} = \frac{1000}{4.05 \times 10^6} = .247 \times 10^{-3}$$

$$C_2 = 7.23 \times 10^{-6}$$

$$\frac{C_2}{2} = 3.61$$

$$\frac{C_2}{18} = .352 \times 10^{-6}$$

$$\frac{C_2}{(18)^2} = .020 \times 10^{-6}$$

$$\frac{C_2}{2(18)^2} = .010 \times 10^{-6}$$

$$\frac{3\ C_2}{(18)^3} = .0005 \times 10^{-6}$$

$$\frac{1}{18} = 55.6 \times 10^{-3}$$

and $\quad S(0) = 1000 \text{ psi} = 10^3 \text{ psi}$.

Substituting the values of the constants gives

$$(46) \quad \delta(t)_{min} = 0.247 \times 10^{-3} + \left[\frac{.352\ t}{t + 18} \quad \frac{6.32\ t}{(t + 18)^2} \right] 10^{-3}$$

and

$$(47) \quad \delta(t)_{max} = 0.247 \times 10^{-3} + 6.32 \times 10^{-6} \times \frac{t}{t + 18} \left[- \frac{3.16}{(t + 18)^2} + \frac{3.16\ (t + 6)}{(t + 18)3} + 55.58 \right].$$

These theoretical bounds are compared to the experimentally determined creep in Fig. 8. Curve A is plotted from actual measurements and represents the gross creep. This graph does not include the elastic deformation $\frac{S}{E}$ because the first measurement was taken after the elastic deformation had taken place.

Curve B is the shrinkage of the control beam, No. 3. When this shrinkage is subtracted from the gross creep of curve A, pure creep is obtained which is represented by curve C.

$\delta_{max}(t)$ and $\delta_{min}(t)$ are the maximum and minimum bounding functions of the total strain $\delta(t)$, which therefore lies between them. In Fig. 9, $\delta_{max}(t) - \frac{S(t)}{E}$ and $\delta_{min}(t) - \frac{S(t)}{E}$, which

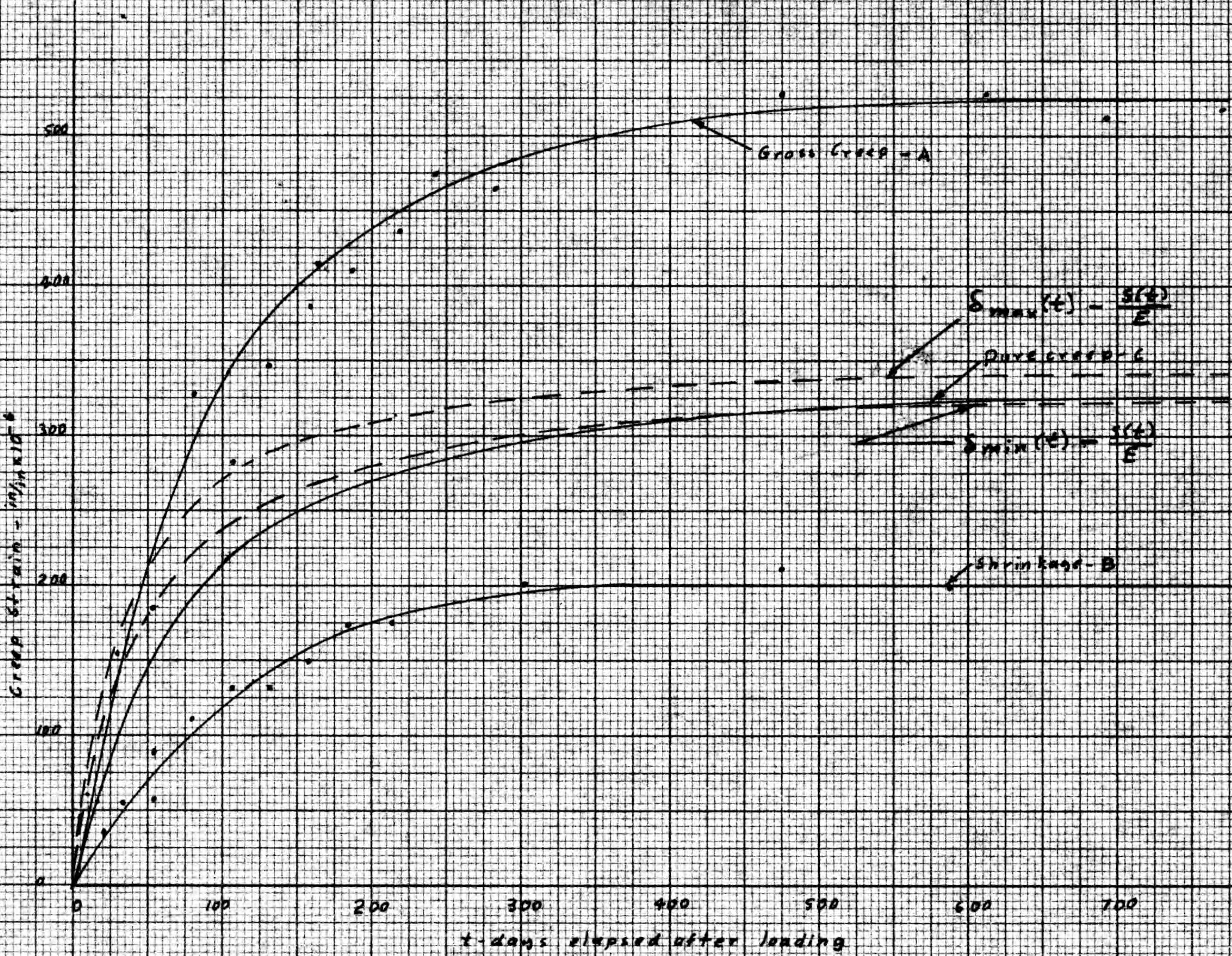

Fig.3. Theoretical and experimental values for beam No.2 .

represent bounding functions for the theoretical creep, are shown for comparison to the experimentally determined values.

It should be noted that although the theoretical and experimental curves have the same general character, there is some deviation for small t. The probable cause for this discrepancy is the difference between the empirical formula (38) for $a(K,t)$ and its true values for small values of K and t as shown in Fig. 7.

Analysis of the Simply Loaded Prestressed Beam

Beam No. 1 was a prestressed beam loaded at the third points as shown below.

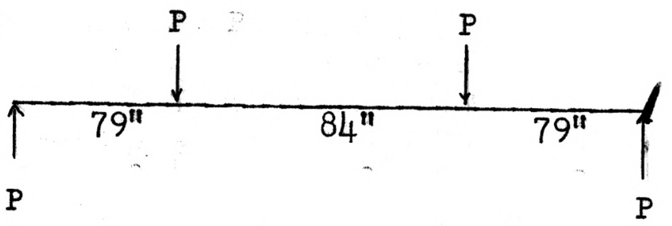

P = 11,500 lbs.

Such a beam is analyzed in problem 3 of the Linearized Creep Theory. This analysis was used to provide a theoretical deflection curve for comparison to the deflections measured in the experiment.

An expression $\Delta(t)$, for the center deflection of the portion of beam No. 1 between the supports, was derived as follows.

From (27) the curvature $\frac{1}{\rho}$ of the beam is approximately

$$\frac{1}{\rho} = \frac{\partial^2 y}{\partial x^2} = C_2(t)$$

The central portion of the beam under consideration is a section of constant bending moment, and therefore of constant radius, as shown below.

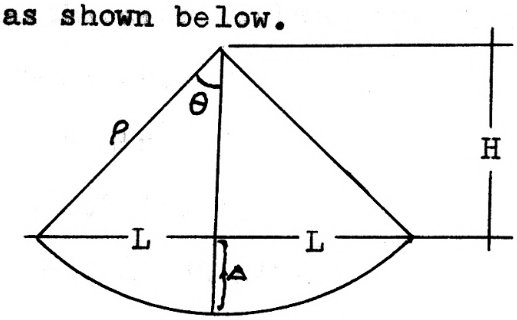

Simple trigonometry and approximation shows

(48) $\rho^2 = L^2 + H^2$,

where $H = \sqrt{\rho^2 - L^2}$,

(49) $\sin\theta = \frac{L}{\rho}$,

(50) $\Delta = \rho\,(1 - \cos\theta)$,

$= \rho\,(1 - \sqrt{\frac{\rho^2 - L^2}{\rho}}$,

$\doteq \rho\,(1 - \sqrt{1 - \frac{L^2}{2}}$

$$\left(1 - (\tfrac{L}{\rho})^2\right)^{1/2} = 1 - \tfrac{1}{2}\,(\tfrac{L}{\rho})^2 ,$$

$= (1 - 1 + \frac{1}{2}\,\frac{L^2}{\rho^2})$,

$\Delta = \frac{L^2}{2\rho}$ and

(51) $\Delta(t) = \frac{L^2}{2\rho\,(t)}$.

Since

$\frac{\partial^2 y}{\partial x^2} \doteq \frac{1}{\rho} \doteq C_2(t)$, it follows that

$\Delta(t) = \frac{L^2}{2}\,C_2(t)$ and

$$(52)\quad \Delta(t) = \frac{L^2}{2}\;\frac{1 + E_c a_c(0,t)}{E_c A_c}\;\frac{\begin{vmatrix} 1 & CO \\ \bar{y} & M(x) + C_O D \end{vmatrix}}{\begin{vmatrix} 1 & \bar{y} \\ \bar{y} & k^2 \end{vmatrix}} .$$

In the case of beam No. 1,

L = 42 in.

$\bar{y}$ = 8 in.

D = 2.5 in.

A_c = 128 sq. in.

$E_c = 3 \times 10^6$ psi.

$M(x) = 920{,}000$ lb-in.

$F. = 66{,}500$ lbs. (initial force on steel)

$$k^2 = \frac{I_c}{A_c} = \frac{\frac{1}{3}\, bh^3}{A_c} = \frac{\frac{1}{3} \times 8 \times \overline{16}^3}{128} = 85.33$$

$k^2 = 85.33$

$$a(K,t) = 0.211 \times 10^{-6}\ \frac{K + 44}{K + 18}\ \frac{t}{t + 18}\ .$$

Since the beam was loaded at an age of 22 days,

$$a(0,t) \text{ is } a(22,t) = 0.211 \times 10^{-6} \cdot \frac{66}{44} \cdot \frac{t}{t + 18}$$

or

$$a(0,t) = 0.346 \times 10^{-6}\ \frac{t}{t + 18}\ .$$

Thus,

$$(52) \quad \Delta(t) = \frac{L^2}{2} \cdot \frac{1 + E_c a_c(0,t)}{E_c A_c} \cdot \frac{M(x) + C_0 D - \bar{y}\, C_0}{k^2 - \bar{y}^2}\ .$$

In this expression it should be noted that C_0, the force in the steel at time t, must be known.

From equation (32),

$$C_0 = \frac{F - R\,(D - \bar{y})\, M(x)}{1 + R\,(k^2 - 2\bar{y}\, D + D^2)}\ ,$$

where

$$R = \frac{1 + E_c a_c(0,t)}{E_c A_c\ (k^2 - \bar{y}^2)}\ E_s A_s\ .$$

The variation C_0 with time is shown in Fig. 9, assuming that the initial force in the cables was 66,500 lbs.

Substituting this value for C_0 into (52) gives

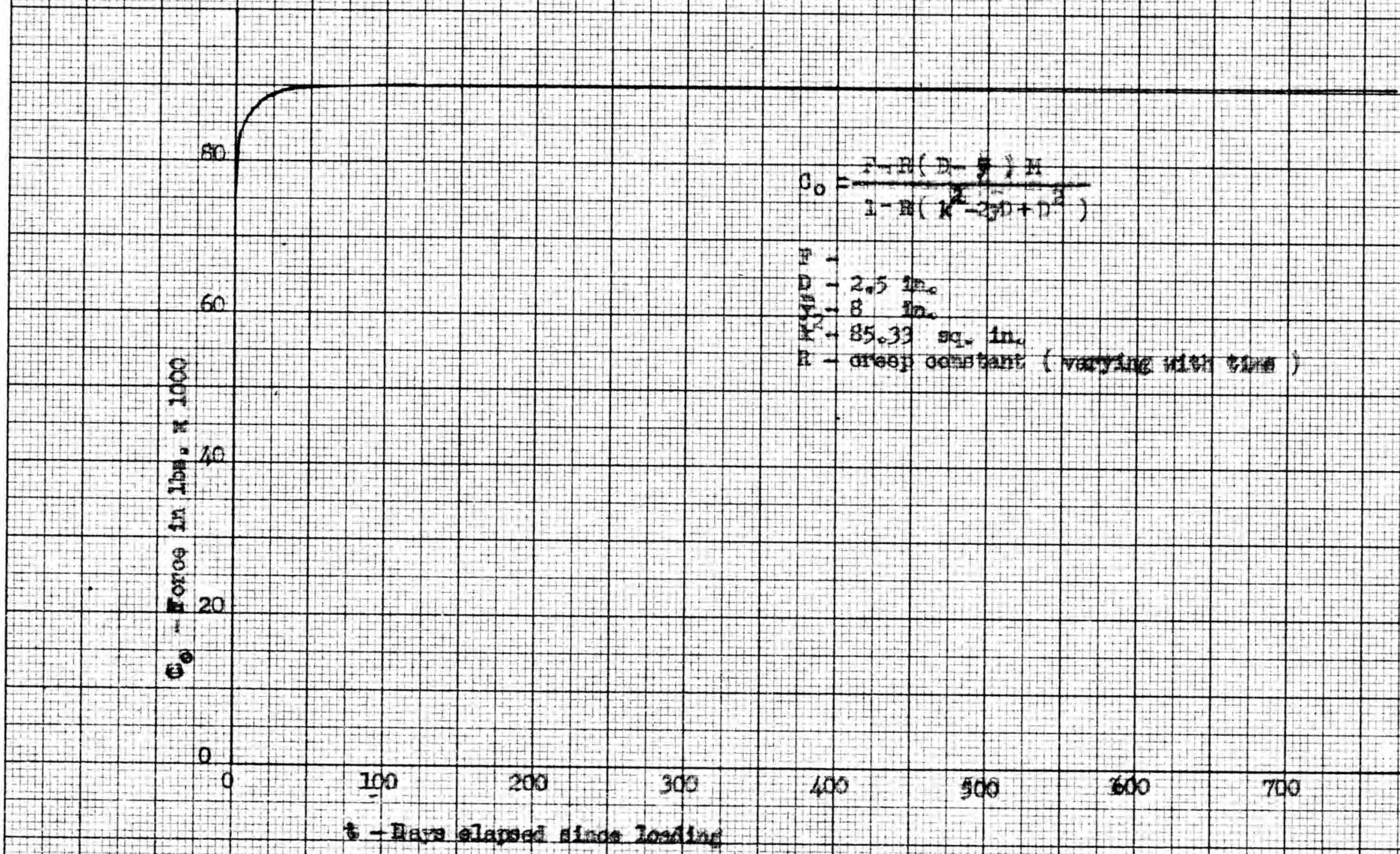

Fig.9.Variation of the force in the prestressing wires of beam No.1 .

$$(53)\quad \Delta(t) = \frac{L^2}{2}\ \frac{R}{E_sA_s}\quad M(x) + (D - \bar{y})\left[\left(\frac{F - R\ (D - \bar{y})\ M(x)}{1 + R\ (k^2 - 2\bar{y}\ D + D^2)}\right)\right].$$

This gives the theoretical deflection of central portion of beam No. 1 when the proper values of the constants are used.

The theoretical deflection curve is compared to the experimental values in Fig. 10.

Experimental Values of $\Delta(t)$

These values are taken from Table in Appendix. They are obtained by averaging the points 3, 7, 12, and 16 and taking the difference between averages of pts. 5 and 14. The elastic deflection value of .065 is added to all of them.

Days t	Deflection $\Delta(t)$
0	.065
3	.065
10	.075
17	.080
31	.090
52	.092
79	.095
107	.097
133	.105
161	.100
189	.102
218	.105
246	.105
279	.102
304	.105
365	.105
384	.100
511	.110
584	.105
711	.110

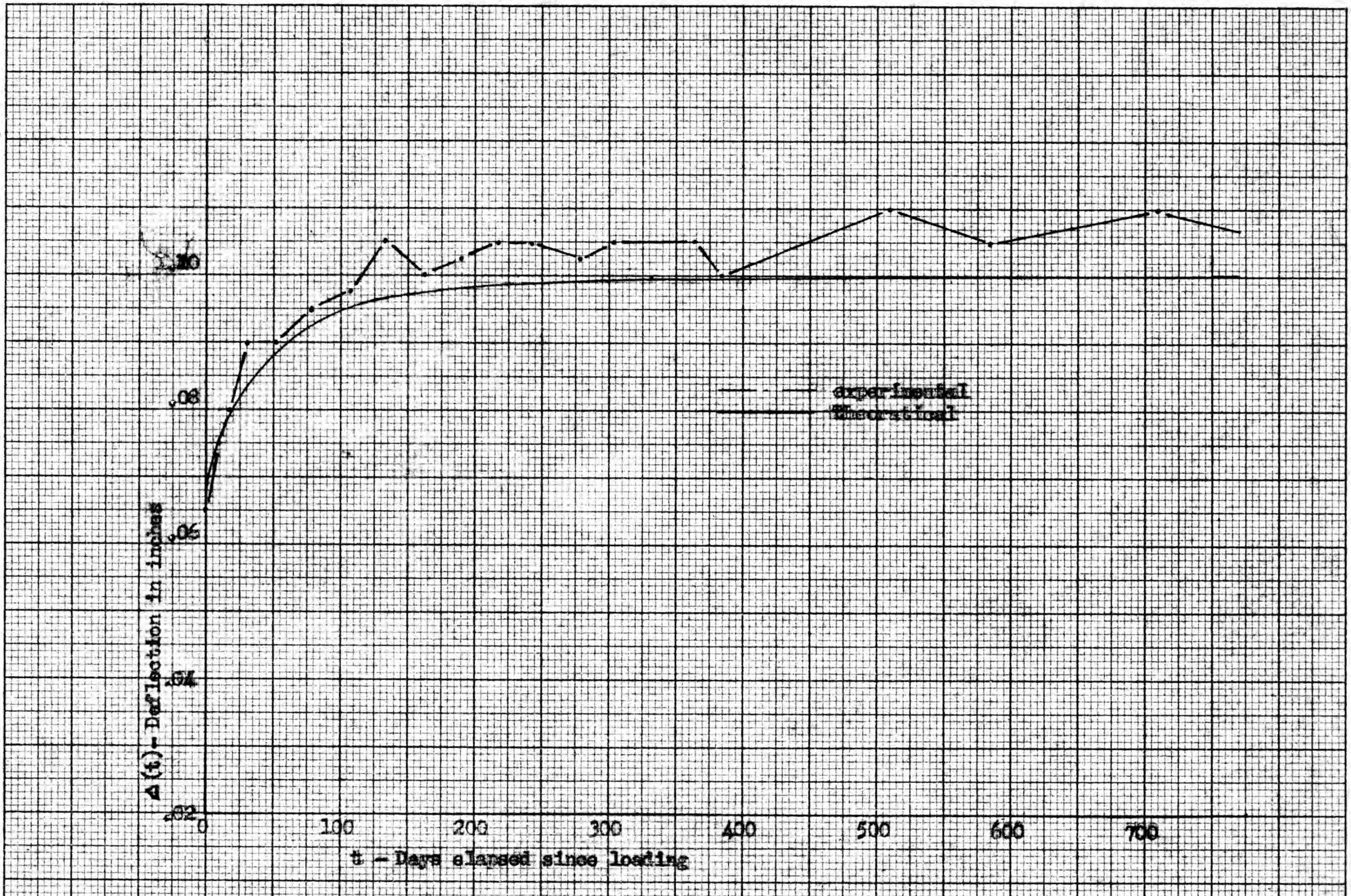

Fig.10. Experimental and theoretical creep curves for beam No.1.

CONCLUDING REMARKS

In general, the linearized creep theory presented here appears to agree both qualitatively and quantitatively with the experimental results obtained from full size beams.

As seen in Fig. 8, the experimental strain measurements of the axially stressed beam agree quite well with those predicted theoretically. The greatest discrepancy occurs at early times t at the region in which the empirical two-dimensional creep function $a(k,t)$ fits the data the poorest.

The agreement between the theoretical and experimental values of the deflection curve $\Delta(t)$ for the laterally loaded beam is even better, as seen from Fig. 10. In this case discrepancies are within the experimental error occurring in the measurement of $\Delta(t)$.

No comparisons between theoretical and experimental strains $\varepsilon(y,t)$ were made for this beam because such comparisons were difficult to make since the experimental measurements were not started at zero strain.

Although the theory seems to check the experimental results quantitatively, several defects occurred in the conduct of the experiment. Those defects were mainly errors of omission made because the experimental work was carried out over a long time, and started without sufficient knowledge and consideration of the linearized theory. The errors themselves allow only qualitative verification of the theory, and are outlined below.

The elastic modulus of elasticity of the concrete, E_c, which occurs frequently in the theoretical analysis, was not determined experimentally. This error is not serious since E_c depends essentially on the elasticity of the constituents of the concrete. The physical properties of concrete supplied by the Walters Sand Company of Manhattan are fairly standard and well known (11).

A more important defect is that the initial force F in the wires was not measured. This value was estimated to make the theoretical deflection curve $\Delta(t)$ check the experimental values quantitatively. This error occurred accidentally because, although the wires were carefully loaded to 140,000 lbs. before the specimens were poured, approximately two days elapsed before the concrete was poured. During this time the force in the wires was supported by two 4" x 1" creosoted bridge planks, under a compressive stress of 1460 psi. It is well known that at this stress wood creeps readily. In fact, after several days under load, one of the bridge planks failed in shear. Creep caused in this manner would reduce the initial force in the steel prestressing cables considerably. The creep of the steel wires themselves is negligable in this case because, as H. Dill showed (5), such creep would occur in several hours. It is estimated that the final load in the prestressing cables was only 48 percent of its original value. Although this value causes the theoretical deflection curve $\Delta(t)$ to agree well with the experimental curve, no more than a qualitative check can be claimed.

A third defect was that strain measuring holes for measurement of $\delta(y,t)$ were not drilled and measured before the prestress wires were cut. Measurements of strain were actually made, but their interpretation is not clear. Although future careful study of the data may be of some value, it probably will not yield conclusive results.

Although the linearized creep theory is at least qualitatively correct, it is fairly complicated, and is not recommended or likely to be used for design. Rather, it should be used to select safe design stresses suitable for use in the usual elementary formulas.

Future research, besides avoiding the errors made in the experiments reported on here, should include further measurements of the creep of concrete to determine its non-linear and recovery characteristics, and attempts at determination of existing forces in wires by careful excavation and measurement of its change of strain on being cut.

ACKNOWLEDGMENTS

The author wishes to express his gratitude to Dr. P. G. Kirmser of the Applied Mechanics Department for his help and guidance, without which this research could not be accomplished.

BIBLIOGRAPHY

(1) Abeles, P. W.
Principles and Practice of Pre-stressed Concrete. London: Crosby Lockwood & Sons, Ltd, 1952.

(2) Arnan, M. A., Reiner, M., and Teinowitz, M.
"Research on Loading Tests of Reinforced Concrete Floor Structures," report of work carried out at the Standards Institutions of Israel, The Research Council of Israel, Jerusalem, 1950. pp. 34-43.

(3) Cowan, H. J.
Inelastic deformation of reinforced concrete in relation to ultimate strength. London: "Engineering," Aug. 1952.

(4) Chubbuck, E. R.
First progress report on pre-stressed beam project (No. 233). Manhattan, Kansas; Dept. of Applied Mechanics, K.S.U., July, 1956.

(5) Dill, H. D.
Relaxation of steel cables used in pre-stressed concrete. Manhattan, Kansas: Dept. of Applied Mechanics, K. S.U. 1957.

(6) Freudenthal, A. M.
The inelastic behavior of engineering materials and structures. New York: John Wiley & Sons, Inc., 1950. pp. 105-107, 523-525.

(7) Investigation of Creep Characteristics of Shasta Dam Concrete.
U. S. Dept. of the Interior, Bureau of Reclamation Concrete Laboratory Report No. C-805, Aug. 9, 1955.

(8) Kirmser, P. G., Private Communication, Kansas State University.

(9) Lorman, W. R.
"The Theory of Concrete Creep," Proceedings, ASTM, V. 40, 1940. p. 1084.

(10) Magnel, G.
Pre-stressed concrete. New York: McGraw-Hill, 1954.

(11) Noble, P. M.
The Effect of Aggregate and Other Variables on the Elastic Properties of Concrete. Kansas State College

Bulletin No. 29; 1932.

(12) Ross, A. D.
"Creep and Shrinkage in Plain, Reinforced, and Prestressed Concrete. A General Method of Calculation." Proceedings, Institution of Civil Engineers. London: V. 21, No. 1, 1943.

(13) Shank, J. R.
"The Plastic Flow of Concrete," Bulletin No. 91, Engineering Experiment Station, Ohio State University, 1935. p. 14.

APPENDIX

Table 1. Properties of the Concrete used.

Constituent:	Wt. :	Abs.Vol. :	Sp. Gr.:	Remarks
Stone	1520	9.36	2.60	Limestone; all pass 3/4"
Sand	1500	9.27	2.60	Concrete sand; pass #4
Cement	658	3.35	3.15	Type I
Water	292	4.75	1.00	
Air	-	0.27	-	1% by vol. assumed
Totals	3970	27.00		

Theor. Unit Wt. = 146.5 lbs. per cu. ft.

Actual Unit Wt. = 145.5 lbs. per cu. ft.

Av. ultimate strength: 4000 psi

Young's Modulus (e) : 4.05×10^6 psi

Table 2. Properties of the pre-stressing cables used.

(a) Nominal diameter = 3/8 inch

(b) Number of strands = 7

(c) Ultimate strength = 20,000 lbs. (250,000 psi)

(d) Net area of wire = 0.0799 sq. in.

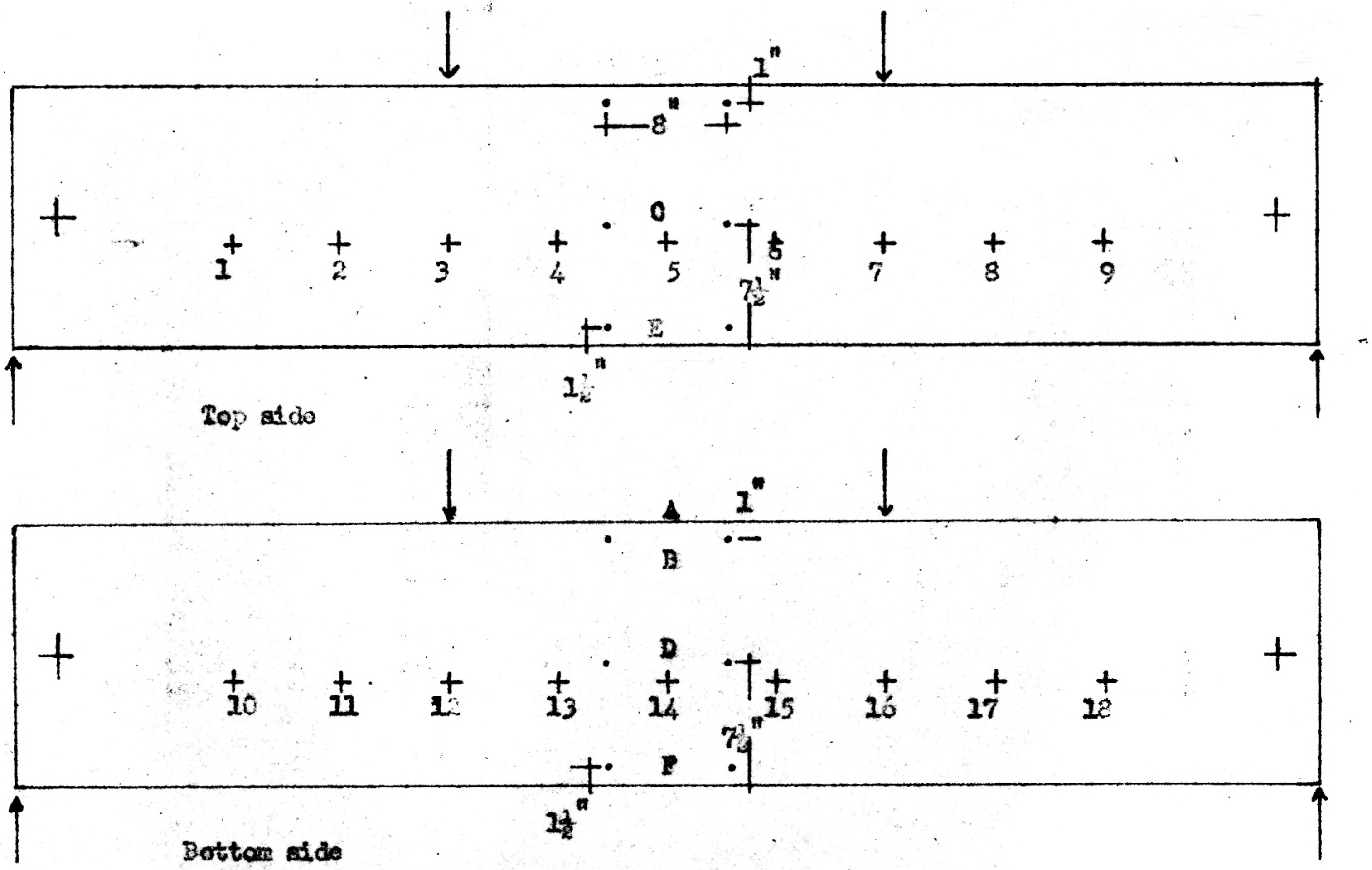

Fig.1. Beam No.1 .

Table 3. Deflection record for beam No. 1

Days	1	2	3	4	5	6	7	8	9	10	11	12	13	14	15	16	17	18	Comments
0	75	94	98	110	90	84	81	77	83	112	89	122	77	97	77	103	103	134	400 psi on each end
0	82	105	114	129	108	103	99	90	90	116	101	139	98	118	99	122	118	140	1000 psi on each end
0	88	119	131	147	127	120	114	102	96	124	113	154	114	135	115	137	128	147	1600 psi on each end*
3	90	122	135	152	131	125	118	105	97	125	115	158	118	139	119	140	131	149	1600 "
10	90	122	136	153	132	126	119	105	97	125	116	159	119	140	121	142	132	150	1475 "
10	92	125	140	156	136	129	123	108	98	127	119	162	123	145	125	145	135	150	1600 "
17	92	125	140	157	137	131	124	108	99	127	120	163	124	145	125	146	135	151	1500 "
17	92	128	143	161	141	134	126	111	100	128	122	167	127	149	128	156	137	152	1600 "
31	93	129	144	163	144	137	129	113	102	130	123	169	131	152	132	151	139	153	1450 "
31	94	130	146	164	145	138	130	113	102	130	125	170	132	152	133	152	140	153	1600 "
52	94	130	147	165	146	139	130	113	102	131	125	171	133	155	134	152	141	153	1500 "
52	94	130	147	165	146	139	130	113	102	131	126	174	136	155	136	155	142	153	1600 "
79	94	130	148	166	147	140	130	113	101	130	125	172	136	155	136	155	141	154	1500 "
79	95	134	150	170	150	142	133	115	101	130	126	173	135	155	135	155	142	153	1600 "
107	94	131	150	167	147	138	132	114	102	132	126	173	137	156	137	156	142	153	1560 "
107	94	131	149	168	148	139	132	114	101	131	127	174	137	156	138	156	142	153	1600 "
133	94	132	150	169	150	143	134	117	102	132	128	177	138	158	139	158	143	156	1550 "
133	95	134	151	169	150	142	131	116	102	131	127	178	140	158	138	158	144	153	1600 "
161	95	133	151	170	151	144	133	115	102	130	127	176	138	158	139	158	143	156	1560 "
161	94	132	150	170	151	143	134	114	102	131	128	177	139	158	139	158	143	155	1600 "
189	95	134	154	173	154	146	139	119	106	132	127	177	139	161	140	160	144	153	1580 "
189	96	134	153	172	153	146	137	118	104	130	129	177	138	160	138	157	142	151	1600 "
218	97	134	152	172	152	145	139	116	103	132	130	179	140	163	141	160	144	155	1590 "
218	96	134	154	173	153	146	137	118	104	131	130	178	140	162	140	160	145	155	1600 "
246	96	134	153	173	152	145	136	117	103	131	130	179	138	162	141	160	144	154	1595 "
246	96	134	153	173	153	146	137	116	103	130	129	178	140	163	140	160	143	154	1600 "
279	96	134	153	173	152	146	137	117	103	131	129	178	140	162	140	160	143	154	1595 "
279	96	134	153	173	153	146	136	116	103	131	129	179	140	162	141	160	144	154	1600 "
304	96	134	152	173	153	146	136	117	102	131	129	177	140	161	140	160	145	155	1600 "
365	97	135	153	174	153	146	136	117	102	132	130	178	141	162	141	160	146	156	1600 "
384	95	134	153	172	153	146	141	121	104	133	129	179	141	163	143	160	144	153	1600 "
511	98	136	156	176	156	149	139	119	103	135	131	180	143	165	143	161	145	153	1600 "
584	96	135	153	175	154	148	138	118	103	132	131	182	144	166	145	164	148	158	1600 "
711	96	135	157	176	160	152	144	120	104	134	132	180	142	170	140	165	150	154	1600 "

*This reading is taken as the zero reading

The elastic deflection, or the deflection before any load is applied, is not recorded in the data. Deflection measurements at 400 psi, 1000 psi, and 1600 psi are recorded. From these three values the elastic deflection can be calculated by using method of least squares.

Let y = stress on the beam

x = deflection reading at the time stress is applied

a and b : constants

$$y_i = ax_i + b$$

$$y_1 = ax_1 + b$$
$$y_2 = ax_2 + b$$
$$y_3 = ax_3 + b$$

at $= 0 \qquad x = -\left(\frac{b}{a}\right)$

Using the matrix theory

$$a = \frac{\begin{vmatrix} \Sigma xy & \Sigma x \\ \Sigma y & 3 \end{vmatrix}}{\begin{vmatrix} \Sigma x^2 & \Sigma x \\ \Sigma x & 3 \end{vmatrix}} \qquad b = \frac{\begin{vmatrix} \Sigma x^2 & \Sigma xy \\ \Sigma x & \Sigma y \end{vmatrix}}{\begin{vmatrix} \Sigma x^2 & \Sigma y \\ \Sigma x & 3 \end{vmatrix}}$$

$$-\frac{b}{a} = \frac{\begin{vmatrix} \Sigma x^2 & \Sigma xy \\ \Sigma x & \Sigma y \end{vmatrix}}{\begin{vmatrix} \Sigma xy & \Sigma x \\ \Sigma y & 3 \end{vmatrix}}$$

The values are taken from Table 3. In our problem onlyh points 3, 7, 12, 16, 5, 14 are needed.

Thus, the values in the matrix for m are:

pt.-3	y	x	x^2	xy
	400	x_1= .98	.96	392
	1000	x_2=1.14	1.30	1140
	1600	x_3=1.31	1.70	2096
Σ	3000	3.43	3.97	3628

pt.-7	y	x	x^2	xy
	400	.81	.65	324
	1000	.99	.98	990
	1600	1.14	1.30	1824
Σ	3000	2.94	2.93	3138

pt.-12	y	x	x^2	xy
	400	1.22	1.49	488
	1000	1.39	1.93	1390
	1600	1.54	2.37	2464
Σ	3000	4.15	5.79	4342

pt.-16	y	x	x^2	xy
	400	1.03	1.06	412
	1000	1.22	1.49	1220
	1600	1.37	1.88	2192
Σ	3000	3.62	4.43	3824

pt.-5	y	x	x^2	xy
	400	.90	.81	360
	1000	1.08	1.17	1080
	1000	1.27	1.61	2032
Σ	3000	3.25	3.59	3472

pt.-14	y	x	x^2	xy
	400	.97	.94	388
	1000	1.18	1.39	1180
	1600	1.35	1.82	2160
Σ	3000	3.50	4.15	3728

Sample calculation:

pt.-3

$$-\frac{b}{a} = \frac{\begin{vmatrix} \Sigma x^2 & \Sigma xy \\ \Sigma x & \Sigma y \end{vmatrix}}{\begin{vmatrix} \Sigma xy & \Sigma x \\ \Sigma y & 3 \end{vmatrix}} = \frac{\begin{vmatrix} 3.97 & 3628 \\ 3.43 & 3000 \end{vmatrix}}{\begin{vmatrix} 3628 & 3.43 \\ 3000 & 3 \end{vmatrix}} \qquad -\frac{b}{a} = \frac{-534}{-594} = 0.90$$

pt.	3	7	12	16	5	14
1st. 1600 psi	1.31	1.14	1.54	1.37	1.27	1.35
$-\frac{b}{a}$	- .98	- .71	- 1.12	- .90	- .77	- .87
	.41	.43	.42	.40	.50	.48

Av. of pts. 5,14	=	.490
Av. of pts. 3, 7, 12, 16	=	.425
Difference	=	.065

Elastic deflection = .065

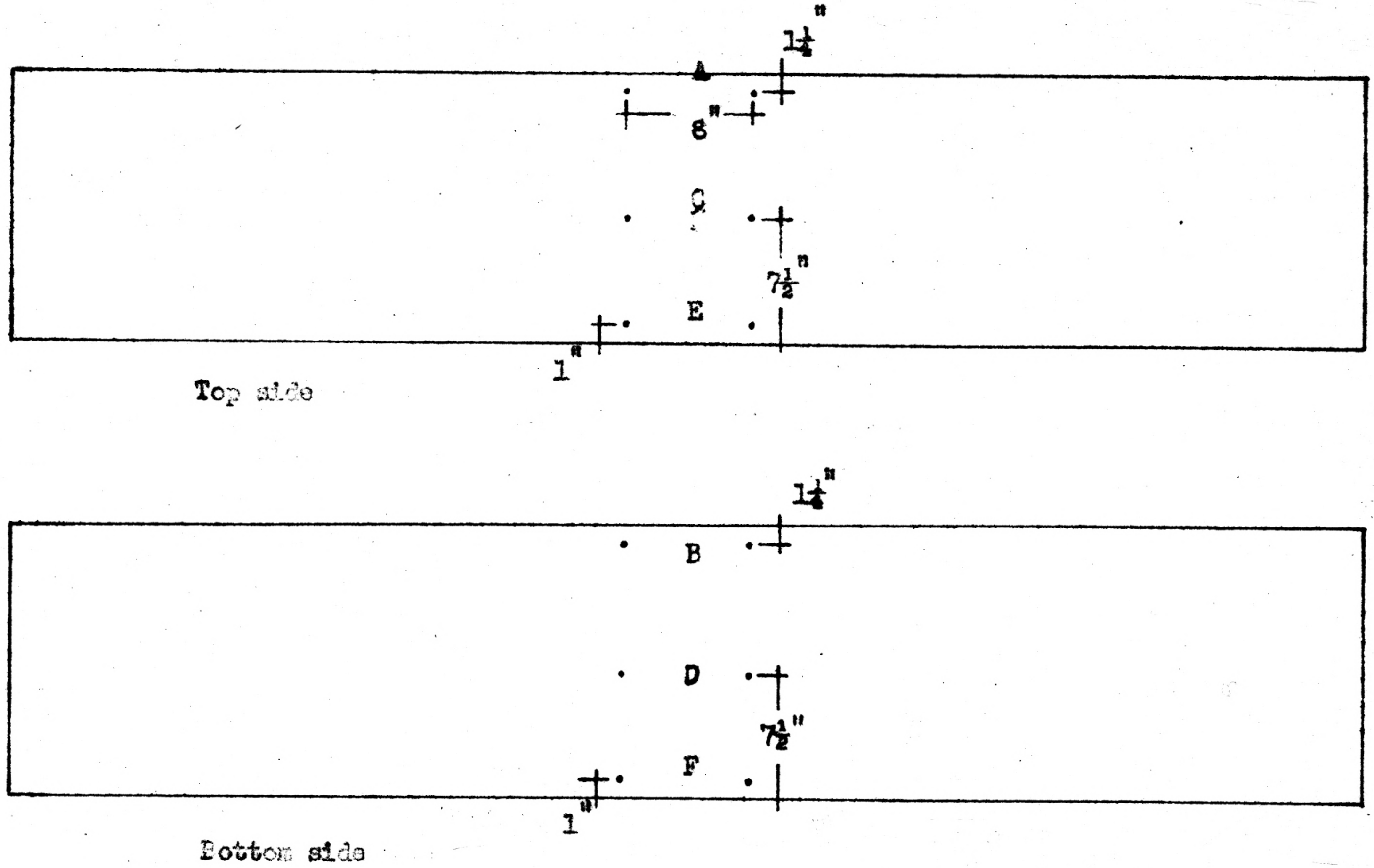

Fig.2. Beams No.2 and No.3 .

Table 4. Strain record for beam No. 1

Days and Temp	Pin Design	Gage Rdgs	Av. Strain (in/inx10^6)	Av. Strain Corr. to 80°	Compl. Corr. Strain	Remarks
	A	542	+406			4000# on each end
0	B	653				(400 psi)
	C	640	+ 19			These strains are
90°F	D	698				with respect to zero
	E	575				Rdgs below.
	F	508	-331			
	A	520	+144			7600# on each end
0	B	633				(1000 psi)
	C	640	+ 13			
90°F	D	597				These strains also
	E	591	-144			with respect to zero
	F	522				rdgs below.
	A	512	0	+21	0	11,500# on each end of
0	B	618				beam (1600 psi on
	C	638	0	+21	0	jack)
90°F	D	597				
	E	602	0	+21	0	This is taken at zero
	F	534				reading.
	A	508	- 44	-23	-44	
3	B	615				
	C	637	+ 6	+27	+ 6	
90°F	D	699				
	E	605	+ 31	+52	+31	
	F	536				
	A	500	-137	-117	-138	1475 psi on jack
10	B	608				each end
	C	631	- 75	- 55	- 76	
89°F	D	692				
	E	601	- 19	+ 1	- 20	
	F	532				
	A	497	-181	-161	-182	1600 psi on jack
10	B	604				each end
	C	631	- 75	- 55	- 76	
89°F	D	692				
	E	603	0	+ 20	- 1	
	F	533				

Table 4. (continued)

Days and Temp	Design	Gage Rdgs	Av. Strain (in/inx10^6)	Av. Strain Corr. to 80°	Compl. Corr. Strain	Remarks
	A	495	-212	-179	-200	1500 psi on jack at each end
17	B	601				
	C	630	- 87	- 54	- 75	
95°F	D	691				
	E	602	0	+ 33	+ 12	
	F	534				
	A	489	-275	-242-	-263	1450 psi on jack at each end
17	B	597				
	C	628	-112	- 79	-100	
95°	D	689				
	E	602	- 6	+ 27	+ 6	
	F	535				
	A	484	-331	-325	-346	1450 psi on jack at each end
31	B	593				
	C	629	-150	-144	-165	
83°F	D	682				
	E	605	- 13	- 7	- 28	
	F	529				
	A	485	-325	-319	-340	1600 psi on jack at each end
31	B	593				
	C	628	-150	-144	-165	
83°F	D	683				
	E	605	- 25	- 19	- 40	
	F	535				
	A	478	-414	-406	-427	1500 psi on jack at each end
52	B	586				
	C	623	-162	-154	-175	
84°F	D	686				
	E	602	0	+ 8	- 13	
	F	534				
	A	478	-414	-408	-429	1600 psi on jack at each end
52	B	586				
	C	623	-169	-163	-184	
83°F	D	685				
	E	601	0	+ 6	- 15	
	F	535				

Table 4. (continued)

Days and Temp	Pin Design	Gage Rdgs	Av. Strain (in/inx106)	Av. Strain Corr. to 80°	Compl. Corr. Strain	Remarks
79	A B	468 575	-544	-530	-551	1500 psi on jack at each end
86.5°F	C D	614 674	-294	-280	-301	
	E F	594 529	- 81	- 67	- 88	
79	A B	466 573	-569	-554	-575	1600 psi on jack at each end
86.5°F	C D	612 675	-300	-286	-307	
	E F	594 529	- 81	- 67	- 88	
107	A B	466 575	-556	-567	-588	Left spring 6.61" Right spring 6.71"
75°F	C D	615 677	-269	-280	-301	1550 psi on jack at each end
	E F	597 530	- 56	- 67	- 88	Temp correction -11 Complete corr. -21
107	A B	466 574	-559	-573	-594	Left spring 6.60" Rt. spring 6.68"
74°F	C D	616 677	-263	-277	-298	1600 psi on jack at each end
	E F	597 532	- 41	- 55	- 76	Temp. corr. -14 Complete corr. -21
133	A B	462 571	-606	-641	-662	Left spring 6.60" Rt. spring 6.68"
64°F	C D	613 673	-306	-341	-362	1550 psi on jack at each end
	E F	596 528	- 75	-110	-131	Temp. Corr. -34 Complete Corr. -21
133	A B	463 570	-600	-641	-662	Left spring 6.60" Rt. spring 6.69"
64°F	C D	614 675	-288	-323	-344	1600 psi on jack at each end
	E F	596 531	- 56	- 91	-112	Temp. corr. -35 Complete corr. -21

Table 4. (continued)

Days and Temp	Pin Design	Gage Rdgs	Av. Strain (in/inx10^6)	Av. Strain Corr. to 80°	Compl. Corr. Strain	Remarks
	A	458	-670	-710	-731	Left spring 6.60"
161	B	565				Rt. spring 6.68"
	C	607	-313	-353	-374	1560 psi on jack
61.5°F	D	678				at each end
	E	593=	-106	-146	-167	Temp. corr. -40
	F	526				Complete corr.-21
	A	459	-656	-696	-717	Left spring 6.59"
161	B	566				Rt. spring 6.68"
	C	609	-344	-384	-405	1600 psi on jack
61.5°F	D	671				at each end
	E	594	-112	-152	-173	Temp. corr. -40
	F	524				Complete corr.-21
	A	455	-694	-754	-775	Left spring
189	B	565				Rt. spring
	C	609	-350	-410	-431	1580 psi on jack
53.5°F	D	670				at each end
	E	594	- 94	-154	-175	Temp. corr. -60
	F	527				Complete corr. -21
	A	455	-693	-753	-774	Left spring 6.56"
189	B	564				Rt. spring 6.63"
	C	609	-338	-398	-419	1600 psi on jack
52.5°F	D	672				at each end
	E	594	-100	-160	-181	Temp. corr. -60
	F	526				Complete corr.-21
	A	451	-743	-765	-786	Left spring 6.56"
218	B	560				Rt. spring 6.66"
	C	606	-381	-403	-424	1590 psi on jack at
70°F	D	668				each end
	E	590	-131	-153	-174	Temp. corr. -22
	F	525				Complete corr. -21
	A	453	-742	-764	-785	Left spring 6.57"
218	B	561				Right spring 6.68
	C	608	-362	-384	-405	1600 psi on jack
70°F	D	669				at each end
	E	591	-131	-153	-174	Temp. corr. -22
	F	524				Complete corr. -21

Table 4. (continued)

Days and Temp	Pin Design	Gage Rdgs	Av. Strain (in/inx10^6)	Av. Strain Corr. to 80°	Compl. Corr. Strain	Remarks
	A	448	-775	-779	-800	Left spring 6.58"
246	B	558				Right spring 6.67"
	C	604	-400	-404	-425	1595 psi on jack
78°F	D	667				at each end
	E	587	-188	-192	-213	Temp. corr. -4
	F	519				Complete corr. -21
	A	447	-795	-799	-820	Left spring 6.56"
246	B	556				Right spring 6.68"
	C	605	-400	-404	-425	1600 psi on jack
78°F	D	666				at each end
	E	587	-182	-186	-207	Temp. corr. -4
	F	520				Complete corr. -21
	A	448	-794	-801	-823	Left spring -6.57"
279	B	555				Right spring -6.68
	C	603	-419	-426	-447	1600 psi on jack
77°F	D	665				at each end
	E	588	-175	-181	-203	Temp. corr. -7
	F	520				Complete corr. -21
	A	447	-800	-814	-835	
304	B	555				
	C	601	-525	-539	-560	
74°F	D	650				
	E	587	-113	-117	-138	
	F	521				
	A	447	-794	-774	-795	1000 psi on jack
366	B	556				at each end
	C	602	-518	-498	-519	
89°F	D	650				
	E	586	-175	-155	-176	
	F	522				
	A	440	-888	-910	-931	1000 psi on jack at
384	B	548				each end
	C	591	-600	-622	-643	
70°F	D	648				
	E	581	-219	-241	-262	
	F	520				

Table 4. (concluded)

Days and Temp	Pin Design	Gage Rdgs	Av. Strain (in/inx10^6)	Av. Strain Corr. to 80°	Compl. Corr. Strain	Remarks
511	A	435	-881	-911	-932	
	B	554				
	C	592	-544	-577	-598	
66°F	D	656				
	E	581	-212	-242	-263	
	F	521				
518	A	432	-963	-989	-1010	1600 psi on jack at each end
	B	544				
	C	592	-575	-598	-619	
68°F	D	651				
	E	578	-244	-267	-288	
	F	519				
584	A	432	-888	-892	-1013	
	B	556				
	C	593	-612	-616	-637	
78°F	D	644				
	E	581	-212	-216	-237	
	F	521				
711	A	435	-938	-942	-963	
	B	545				
	C	592	-631	-635	-656	
72°F	D	642				
	E	583	-206	-210	-231	
	F	520				

Table 5. Strain record for beam No. 2

Days and Temp	Pin Design	Gage Rdgs	Av. Strain $(in/in \times 10^6)$	Av. Strain Corr. to 80°	Compl. Corr. Strain	Remarks
	A	529	0	+21	0	These are the original readings.
0	B	665				
	C	692	0	+21	0	The wires are released.
90°F	D	546				
	E	613	0	+21	0	
	F	747				
	A	630	-19	+ 2	-19	Temp. corr. of +21 added to
3	B	661				
	C	695	+50	+70	+50	
90°F	D	551				
	E	615	+19	+40	+19	
	F	748				
	A	625	-69	-49	-70	Temp corr. = +20
13	B	658				Compl corr. = -20
	C	688	-37	-17	-38	
85°F	D	544				
	E	608	-62	-42	-63	
	F	742				
	A	623	-94	-61	-82	Temp corr. = +33
17	B	656				Compl corr. = -21
	C	687	-44	-11	-32	
95°F	D	544				
	E	606	-56	-23	-44	
	F	745				
	A	621	-131	-125	-146	Temp corr. = + 6
31	B	652				Compl corr. = -21
	C	683	- 87	- 81	-102	
83°F	D	541				
	E	595	-194	-188	-209	
	F	734				
	A	616	-169	-161	-182	Temp corr. = + 8
52	B	651				Compl corr. = -21
	C	679	-138	-130	-151	
84°F	D	537				
	E	598	-206	-198	-219	
	F	729				

Table 5. (continued)

Days and Temp	Pin Design	Gage Rdgs	Av. Strain (in/inx10⁶)	Av. Strain Corr. to 80°	Compl. Corr. Strain	Remarks
79	A	609				
	B	643	-287	-273	-294	Temp corr. = +14 Compl corr. = -21
	C	671				
86.5°F	D	530	-231	-217	-238	
	E	588				
	F	702	-437	-423	-444	
107	A	611				
	B	645	-236	-247	-268	Temp corr. = -11 Compl corr. = -21
	C	673				
74°F	D	529	-225	-236	-257	
	E	589				
	F	720	-319	-330	-351	
133	A	610				
	B	642	-263	-298	-319	Temp corr. = -35 Compl corr. = -21
	C	671				
64°F	D	528	-244	-279	-300	
	E	586				
	F	717	-356	-391	-412	
161	A	605				
	B	637	-325	-365	-385	Temp corr. = -40 Compl corr. = -21
	C	666				
61.5°F	D	525	-294	-334	-355	
	E	575				
	F	712	-456	-496	-507	
189	A	607				
	B	638	-307	-367	-388	Temp corr. = -60 Compl corr. = -21
	C	667				
53°F	D	525	-287	-347	-368	
	E	582				
	F	713	-406	-466	-487	
218	A	603				
	B	635	-350	-372	-393	Temp corr. = -22 Compl corr. = -21
	C	663				
70°F	D	520	-344	-366	-387	
	E	577				
	F	707	-475	-497	-518	

Table 5. (continued)

Days and Temp	Pin Design	Gage Rdgs	Av. Strain (in/inx10^6)	Av. Strain Corr. to 80°	Compl. Corr. Strain	Remarks
	A	599	-405	-409	-430	Temp corr. = -4
246	B	630				Compl corr. = -21
	C	661	-375	-379	-400	
78°F	D	517				
	E	570	-550	-554	-575	
	F	702				
	A	600	-388	-305	-416	Temp Corr. = -7
279	B	632				Compl corr. = -21
	C	661	-312	-319	-440	
77°F	D	517				
	E	570	-500	-507	-528	
	F	710				
	A	599	-400	-412	-433	
304	B	631				
	C	661	-363	-375	-396	
74°F	D	519				
	E	569	-570	-575	-596	
	F	700				
	A	601	-382	-362	-383	
366	B	632				
	C	662	-356	-336	-357	
89°F	D	519				
	E	571	-556	-536	-557	
	F	701				
	A	600	-444	-466	-487	
384	B	623				
	C	659	-400	-422	-443	
70°F	D	515				
	E	567	-600	-622	-643	
	F	697				
	A	599	-450	-480	-501	
518	B	623				
	C	658	-413	-443	-464	
66°F	D	514				
	E	564	-563	-593	-614	
	F	706				

Table 5. (conclusion)

Days and Temp	Pin Design	Gage Rdgs	Av. Strain (in/inx10^6)	Av. Strain Corr. to 80°	Compl. Corr. Strain	Remarks
584	A	597	-463	-463	-484	
	B	623				
78°F	C	659	-425	-429	-450	
	D	511				
	E	565	-563	-567	-588	
	F	705				
711	A	599	-456	-474	-495	
	B	622				
72°F	C	660	-394	-412	-433	
	D	515				
	E	568	-575	-583	-604	
	F	700				

Table 6. Strain record for beam No. 3

Days and Temp	Pin Design	Gage Rdgs	Av. Strain (in/inx10^{6})	Av. Strain Corr. to 80°	Compl. Corr. Strain	Remarks
0	A	640	0	+21	0	This is original reading.
	B	428				
90°F	C	551	0	+21	0	
	D	675				
	E	687	0	+21	0	
	F	740				
3	A	642	0	+21	0	
	B	426				
90°F	C	553	+19	+40	-2	
	D	676				
	E	691	+19	+40	-2	
	F	739				
13	A	637	-81	-62	-83	
	B	418				
89°F	C	549	-31	-12	-33	
	D	672				
	E	688	-19	- 0	-21	
	F	735				
17	A	635	-63	-30	-51	
	B	423				
95°	C	548	-37	- 4	-25	
	D	672				
	E	687	-44	-11	-33	
	F	733				
31	A	635	-56	-50	-71	
	B	424				
83°F	C	549	-56	-50	-71	
	D	668				
	E	686	-44	-38	-59	
	F	734				
52	A	632	-100	-92	-113	
	B	420				
84°F	C	547	-44	-36	-57	
	D	672				
	E	685	-37	-29	-50	
	F	736				

Table 6. (continued)

Days and Temp	Pin Design	Gage Rdgs	Av. Strain (in/inx10^6)	Av. Strain Corr. to 80°	Compl. Corr. Strain	Remarks
	A	627	-94	-80	-101	
79	B	426				
	C	542	-119	-105	-126	
86.5°F	D	665				
	E	679	-144	-130	-151	
	F	725				
	A	630	-119	-130	-151	Temp corr. = -11
107	B	419				Complete corr. 27
	C	544	-81	-92	-123	
75°F	D	669				
	E	683	-75	-86	-107	
	F	732				
	A	630	-131	-166	-187	Temp corr. = -35
133	B	417				Compl corr. = 21
	C	544	-94	-129	-150	
64°	D	667				
	E	681	-87	-122	-133	
	F	732				
	A	627	-131	-171	-193	Temp corr. = -40
161	B	420				Compl corr. = 21
	C	541	-181	-221	-242	
61°F	D	656				
	E	678	-143	-183	-204	
	F	726				
	A	629	-150	-210	-231	Temp corr. = -60
189	B	425				Compl corr. = 21
	C	543	-113	-173	-194	
53°F	D	665				
	E	679	-106	-166	-187	
	F	731				
	A	625	-132	-154	-175	Temp corr. = -22
218	B	422				Compl corr. = 21
	C	535	-144	-166	-187	
70°F	D	664				
	E	677	-150	-172	-193	
	F	726				

Table 6. (continued)

Days and Temp	Pin Design	Gage Rdgs	Av. Strain (in/inx10^6)	Av. Strain Corr. to 80°	Compl. Corr. Strain	Remarks
246	A	623	-175	-179	-190	Temp corr. = -4
	B	417=				Compl corr. = 21
	C	537	-235	-235	-260	
78°F	D	653				
	E	679	-163	-170	-191	
	F	723				
279	A	624	-181	-189	-210	Temp corr. = -7
	B	415				Compl corr. = 21
	C	538	-212	-219	-240	
77°F	D	654				
	E	677	-163	-170	-191	
	F	724				
304	A	624	-194	-208	-229	Temp corr. = -14
	B	413				Compl corr. = 21
	C	538	-230	-244	-265	
74°F	D	655				
	E	674	-175	-189	-210	
	F	725				
366	A	628	-163	-143	-164	Temp corr. = 20
	B	414				Compl corr. = 21
	C	541=	-181	-161	-182	
89°F	D	656				
	E	677	-150	-130	-151	
	F	726				
384	A	628	-188	-210	-231	Temp corr. = 22
	B	410				Compl corr. = 21
	C	542		- 91	-102	
70°F	D	*673				
	E	676	-156	-178	-199	
	F	726				
398	A	629	-183	-213	-234	*It was noticed that there was a hairline crack due to lifting the beam, and D rdgs should be disregarded.
	B	410				
	C	542				
66°F	D	*670				
	E	678	-150	-180	-203	
	F	725				

Table 6. (continued)

Days and Temp	Pin Design	Gage Rdgs	Av. Strain (in/inx10^6)	Av. Strain Corr. to 80°	Compl. Corr. Strain	Remarks
571	A					
	B	398				
	C					
66°F	D	*656				
	E					
	F	715				
	A	631				
518	B	410	-169	-199	-220	
	C	544				
66°F	D	671				
	E	680	-169	-199	-220	
	F	722				
	A	629				
	B	412	-169	-173	-194	
	C	541				
	D	*670				
	E	676				
	F	689				

Table 7. Strain record for small specimens (3" x 4" x 16")

Days and Temp	Ident	Conc. Stress	Gage Rdgs S-1	Gage Rdgs S-2	Cum. Strains Gross	Gross Av.	Shrink	Shrink Av.	Creep	Creep Av.
21	1	0	638	642			0	0		
	2	0	527	651			0			
90°F	3	0	623	598	-281	-268				-268
	4	0	600	632	-256					
	5	0	594	633	-438	-438				-438
	1	0	638	642						
21	2	0	527	651						
	3	1000	603	573						
90°F	4	1000	579	612						
	5	1500	560	597						
	1	0	632	640			50	103		
25	2	0	517	636			156			
	3	1000	586	551	244	247			141	144
90°F	4	1000	559	592	250				147	
	5	1500	534	568	344	344				241
	1	0	631	635			87	141		
28	2	0	516	631			104			
	3	1000	581	545	312	315			171	175
90°F	4	1000	554	586	319				178	
	5	1500	526	560	444	444				303
	1	0	621	626			206	244		
38	2	0	507	626			281			
	3	1000	565	528	526	535			282	291
89°F	4	1000	537	571	544				300	
	5	1500	508	538	694	694				694
	1	0	616	626			236	278		
42	2	0	503	624			319			
	3	1000	560	521	594	600			316	322
95°F	4	1000	530	564	606				328	
	5	1500	500	530	795	795				517
	1	0	616	620			275	307		
56	2	0	504	620			338			
	3	1000	554	515	670	683			363	376
83°F	4	1000	523	557	698				388	
	5	1500	491	520	912	912				605

Table 7. (continued)

Days and Temp	Ident	Conc. Stress	Gage Rdgs S-1	Gage Rdgs S-2	Cum. Strains Gross	Gross Av.	Shrink	Shrink Av.	Creep	Creep Av.
	1	0	609	612			369	394		
77	2	0	498	613			419			
	3	1000	542	502	826	839			432	445
84°F	4	1000	510	545	852				458	
	5	1500	476	504	1110	1110				716
	1	0	594	609			481	472		
104	2	0	494	610			462			
	3	1000	536	494	912	928			440	455
86.5°F	4	1000	502	538	942				470	
	5	1500	469	495	1207	1207			835	835
	1	0	607	612			382	400		
132	2	0	497	614			419			
	3	1000	537	495	900	916			500	516
75°F	4	1000	503	539	932				532	
	5	1500	468	494	1220	1220				820
	1	0	607	611			388	407		
158	2	0	498	612			425			
	3	1000	535	493	926	941			519	534
64°F	4	1000	501	537	955				548	
	5	1500	466	485	1285	1285			878	878
	1	0	605	605			437	441		
186	2	0	496	611			444			
	3	1000	533	496	920	951			483	510
61.5°F	4	1000	499	535	981				537	
	5	1500	465	483	1306	1306			865	865
	1	0	608	611			381	406		
214	2	0	496	613			431			
	3	1000	533	492	944	969			563	563
52.5°F	4	1000	498	534	944				563	
	5	1500	463	482	1325	1325			919	919
	1	0	603	611			413	450		
243	2	0	491	609			487			
	3	1000	530	488	988	1007			538	557
57°F	4	1000	495	532	1025				575	
	5	1500	461	479	1300	1300			950	950

Table 7. (continued)

Days: and Temp	Ident	Conc. Stress	Gage Rdgs S-1	Gage Rdgs S-2	Cum. Strains Gross	Gross Av.	Shrink	Shrink Av.	Creep	Creep Av.
	1	0	605	606			431			
271	2	0	491	610			475	453		
	3	1000	534	490	950				497	553
78°F	4	1000	493	528	1062	1006			609	
	5	1500	460	484	1333					880
	1	0	605	608			419			
304	2	0	493	610			469	444		
	3	1000	535	491	938				494	
77°F	4	1000	494	529	1050	994			606	550
	5	1500	461	484	1325	1325				881
	1	0	607	610			394			
329	2	0	494	612			450	427		
	3	1000	536	493	920				493	
74°F	4	1000	495	530	1038	979			611	552
	5	1500	461	484	1327					900
	1	0	612	610			362			
391	2	0	498	616			400	381		
	3	1000	541	496	869				488	
89°F	4	1000	500	534	982	925			601	544
	5	1500	464	489	276					895
	1	0	606	605			430			
509	2	0	493	612			456	443		
	3	1000	527	483	1031				588	
70°F	4	1000	492	528	1069	1050			623	607
	5	1500	456	473	1425					982
	1	0	606	605			430			
741	2	0	495	611			456	443		
	3	1000	532	488	975	1038			532	
66°F	4	1000	491	524	1100				657	580
	5	1500	456	472	1431					988
	1	0	605	605			438			
817	2	0	493	611			463	451		
	3	1000	530	489	982					
78°F	4	1000	488	522	1132	1057			531	606
	5	1500	456	474	1420				681	969

Table 7. (concluded)

Days and Temp	Ident	Conc. Stress	Gage Rdgs S-1	Gage Rdgs S-2	Cum. Strains Gross	Gross Av.	Shrink	Shrink Av.	Creep	Creep Av.
	1	0	612	610			362			
924	2	0	498	612			425	394		
	3	1000	526	490	1000	1032			606	638
72°F	4	1000	493	528	1063				669	
	5	1500	454	478	1408					1014

Sample calculation: (at 25 days) =

$$\frac{[1280 - (632 + 640)] \times 10^{-4}\text{in.}}{2 \times 8 \text{ in.}} = 50 \times 10^{-6} \text{ in/in.}$$

CREEP AND PRE-STRESSED CONCRETE

by

ATILLA ORHUN

B.S., Robert College, Istanbul, Turkey, 1957

AN ABSTRACT OF A THESIS

submitted in partial fulfillment of the

requirements for the degree

MASTER OF SCIENCE

Department of Civil Engineering

KANSAS STATE UNIVERSITY
OF AGRICULTURE AND APPLIED SCIENCE

1960

ABSTRACT

The primary purpose of this investigation was to compare the theoretical creep behavior of full sized prestressed concrete beams, as predicted by a linearized creep theory using data obtained from small specimens, to this actual creep behavior as determined by experiment.

To verify this theory, developed by Professor P. G. Kirmser of the Applied Mechanics Department, Kansas State University, two full sized prestressed beams, one full sized prestressed post, and four small compression specimens were cast from one batch of concrete, and subjected to long time constant loads.

Lateral deflections and longitudinal strains were measured over a period of nearly three years, and these experimental values were compared to the theoretical ones computed using the linearized creep theory and the creep properties measured from the small specimens.

Although the theoretical predictions are in excellent agreement with experimental measurements, the theory is checked only qualitatively because of several defects in the conduct of the experiment. The causes and effects of these experimental errors are discussed.

The linearized theory may be too complicated for general use. However, it appears that future study may yield suitable design values for use in the simpler stress theories now in common use.